NTNU
Det skapende universitet

Analytical Solution To Transient Flow in Stress-Sensitive Reservoirs with Pressure Dependent Variables

Karoline B Lillehammer

Petroleumsfag
Innlevert: juli 2015
Hovedveileder: Tom Aage Jelmert, IPT

Norges teknisk-naturvitenskapelige universitet
Institutt for petroleumsteknologi og anvendt geofysikk

Acknowledgments

This thesis was completed at the Norwegian University of Science and Technology (NTNU), in the Department of Petroleum Engineering and Applied Geophysics. I would like to thank my supervisor, Tom Aage Jelmert, who has been very helpful and supported me with his insights throughout the semester. I would also like to thank my friends for keeping my morale high and helping me reach my goal in completing the thesis. Lastly a special thanks to my family for all their support both motivational and by proofreading. Without all of you this would not have been possible.

Trondheim 2015, Karoline Blyberg Lillehammer

Summary

New technology and knowledge gives increasing confidence in investments of unconventional reservoirs. In these types of reservoirs the rock and fluid parameters are often seen to depend strongly on pressure. Conventional well testing equations do not account for stress-sensitivity and assume all reservoir and fluid parameters to be constant. This thesis will suggest a new solution for transient flow by extending the diffusivity equation where pressure dependency of permeability, viscosity, compressibility and thickness is included.

The diffusivity equation becomes strongly non-linear when including pressure dependent parameters. All the pressure dependent variables are assumed to vary exponentially with pressure. Using these exponential relations the model incorporates the pressure dependent variables into a single pressure dependent variable T_n. The normalized transmissibility variable, T_n is a pressure dependent variable and a function of the combined dimensionless elasticity modulus, τ_D, used to describe the degree of stress-sensitivity. Introducing T_n enables the equation to be solved analytically, creating a model that intends to provides better prediction of pressure and flow behavior for stress-sensitive reservoirs.

Special attention is given to the pressure dependency of the reservoir thickness near the well and it is found that stress-sensitivity can cause deformation here. This deformation is found both for the case of drawdown and buildup pressures. It is observed that the deformation during drawdown is larger than the reversed deformation during buildup. By increasing the degree of stress-sensitivity both these phenomenons are also found to increase. From the buildup solution it can thereby be concluded that not all deformation can be reversed by increasing pressure. Hence it indicates the importance of being able to predict deformation early in the life of a field, so that pressure support can be applied before deformation becomes irreversible.

The derived analytical equations are incorporated into well tests to compare against homogeneous solutions. A deviation from homogeneous values is found for all well test cases. The model can also account for storage and skin by the use of Laplace space solutions. The stress sensitivity has little effect on the early time unit slope for storage. Adding skin causes an extra pressure increase at intermediate and late times.

Sammendrag

Ny teknologi og kunnskap gir økt trygghet for investeringer i ukonvensjonelle reservoarer. Formasjons- og fluidparametere i slike reservoarer er ofte sterkt trykkavhengige. Konvensjonelle ligninger i brønntesting tar ikke høyde for spenningsfølsomhet og ofte antas alle reservoar- og fluidparametre konstante. Denne masteroppgaven vil foreslå en ny løsning for transient strømning ved å utvide diffusjonsligningen slik at den inkluderer trykkavhengighet av permeabilitet, viskositet, kompressibilitet og tykkelse.

Diffusjonsligningen blir sterkt ikke-lineær når trykkavhengige parametere inkluderes. Alle trykkavhengige variablene er antatt å variere eksponentielt med trykk. Ved hjelp av disse eksponentielle relasjonene kan modellen inkludere de trykkavhengige variablene inn i én avhengig variabel,T_n. Den normaliserte transmissibilitetsvariabelen, T_n er en trykkavhengig variabel, avhengig av den kombinerte dimensjonsløse elastisiteten,τ_D, som brukes for å beskrive graden av spenningssensitivitet. Ved å introdusere variabelen T_n kan ligningen løses analytisk og en kan dermed opprette en modell som gir bedre prediksjoner av trykk og strømningsadferd.

Det er tatt spesiellt hensyn til reservoartykkelsens trykkavhengighet nær brønnen og det observeres at spenningsfølsomhet kan forårsake noe deformasjon her. Denne deformasjonen er funnet både for tilfellet av nedsynkningstrykk og oppbyggingstrykk. Det er observert at deformasjonen ved synkende trykk er større enn den reverserte deformasjonen ved økende trykk. Ved å øke graden av spenningsfølsomhet forsterkes også disse to fenomenene. Fra oppyggningstrykkløsningen kan det derfor konkluderes med at ikke all deformasjon kan reverseres ved å øke trykket. Det er altså viktig å kunne forutsi deformasjon tidlig slik at trykkstøtte kan tilføres før deformasjonen blir irreversibel.

De utledede analytiske likningene anvendes for å uttrykke brønntestkurver og sammenligne resultatene mot homogene løsninger. Avvik fra homogene verdier er funnet for alle brønntestkurver. Modellen kan også omfatte brønnlagring og skinfaktor ved bruk av Laplace transformasjon. For brønnlagring kan det se ut som om spenningssensitiviteten har liten effekt på den tidlige engetshelningen. Ved å inkludere skinfaktor vil trykket ved senere tid øke mer enn for den homogene løsningen.

Contents

List of Tables

List of Figures

Chapter 1

Introduction

1.1 Motivation

The depletion of reservoirs and the following subsidence due to pressure decrease cause the effective stress on the matrix to increase leading to the change in reservoir properties. For conventional reservoirs this effect is considered small, and average properties for rock and fluid can be assumed. For a stress-sensitive reservoir the assumption of constant properties is not valid. Properties like permeability, viscosity, fluid density and reservoir height are believed to be highly dependent on pressure. These pressure dependencies have to be incorporate into well test equations so that new and hopefully more accurate predictions can be made. The model represented is appropriate for new fields, where the information of reservoir parameters is scarce. When stress-sensitivity is known to be present in a field, early and accurate predictions of the well performance are essential. Improving well test models for the case of pressure dependency on rock and fluid parameters is therefor believed to be important.

1.2 Goal

The main goal of this thesis will be to develop a new set of equations describing transient flow in a stress-sensitive reservoir with several pressure dependent variables. The first focus will be on building a model for the drawdown solution, before expanding to find the buildup solution and a solution including storage and skin. Special attention will be

paid to the change in reservoir thickness at the well, and how it may behave under pressure reduction and increase. Several ways to obtain solutions to the suggested equations will be investigated and presented, depending on level of accuracy and implementation difficulty wanted.

1.3 Approach and Organization

This thesis will describe an analytical approach to solving the diffusivity equation when several rock and fluid parameters are assumed to be pressure dependent. A new set of solutions to be used for well testing in stress-sensitive reservoirs is derived. The new solutions is used to investigate possible compaction near the well and then compared to already existing stress-sensitive and homogeneous cases. An extensive literature and theory review is done on relevant topics.

The thesis will be organized as follows:

- Chapter 2 gives an introduction to relevant well testing theory and well testing curves that are compared and analyzed against the new solution in the results chapter (Chapter 6).
- Chapter 3 contains a literature review of stress-sensitive reservoirs, pressure dependent variables and different approaches of obtaining transient solutions in the case of stress-sensitivity.
- Chapter 4 gives an overview of the mathematical theory needed to solve the diffusivity equation when non-linear, as for the case with pressure dependent variables.
- Chapter 5 represents the derivation of the new suggested analytical solution.
- Chapter 6 describes the results obtained investigating the deformation caused by drawdown and buildup pressures. The sensitivity of the analytical solution is also considered, comparing degrees of stress-sensitivity against the homogeneous case by well tests curves.
- Chapter 7 further discusses the results obtained and represents suggestions for further work.
- Chapter 8 concludes the thesis and summarizes findings drawn form the work.

Chapter 2

Basic Well Testing Theory

The basic purpose of a well test is to create a transient pressure response that causes the formation fluids to enter the wellbore. By monitoring pressure and flow rate one may obtain important information to characterize the well and reservoir, Lee (1982). Together with geological, geophysical and petrophysical information simulation models to predict the reservoir behavior and the expected fluid recovery can be made.

Usually pressure is recorded downhole at the well and the flow rate measured at the surface, Bourdet (2002). As the well is flowing the drawdown pressure response is recorded and as the well is shut in the build up pressure behavior is consequently measured. The pressure and flow rate behavior for flowing and shut in period are illustrated in figure 2.1.

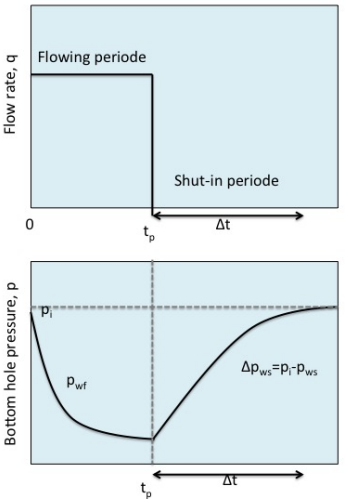

Figure 2.1: Illustrative pressure and flowrate responses for a drawdown and buildup test sequence.

In the ideal case, as illustrated in figure 2.1, the well should be producing at constant rate during drawdown. In reality this is difficult to achieve and may often lead to difficulties in analysing the pressure data from the drawdown period, Lee (1982).

When the well is shut in and the pressure build up test is recorded, the flow rate can be

accurately controlled, as it is zero. It is important that a constant rate is achieved before performing a build up test. The pressure increase during build up often gives more reliable pressure data.

From the pressure data the permeability, both horizontal and vertical, reservoir heterogeneities, boundaries and pressures can be found. The productivity index and the geometry of the well can also be found. All these parameters give important information both for exploration, appraisal and development wells, Bourdet (2002).

2.1 Flow Regimes

The fluid flow and pressure behavior with respect to time is divided into three main types. The different flow regimes are illustrated in figure 2.2 with their corresponding mathematical expressions.

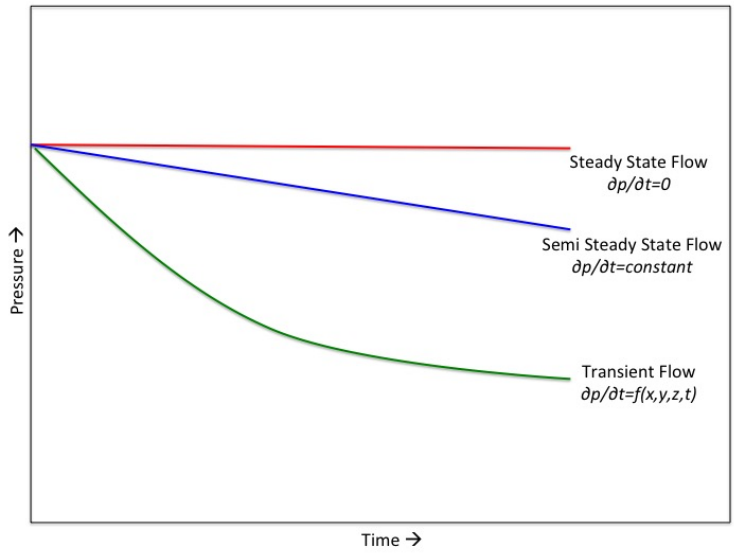

Figure 2.2: Difference in behavior with pressure and time for the three main types of flow regimes.

Steady state

In steady state flow the pressure does not change with time and thereby remains constant at every location in the reservoir, Ahmed (2001). The pressure variation with time is

dependent on the reservoir properties as well as the geometry of the well.

Semi steady state

In semi steady state flow, also known as pseudo steady flow, the pressure declines at a constant rate with respect to time. This corresponds to a closed system response.

Transient flow

In transient flow the pressure is non-zero or constant at any location in the reservoir. The variation in pressure with time is dependent of the reservoir properties as well as the geometry of the well, Ahmed (2001). This flow regime is the most relevant for this study, and is investigated based on the diffusivity equation.

2.2 The Diffusivity Equation

The diffusivity equation describes flow towards a well in a certain reservoir geometry by combining Darcy's law and the law for conservation of mass, Lee (1982). The equation assumes single-phase isothermal flow with small and constant compressibility. For radial flow from a circular reservoir, the diffusivity equation is expressed as follows

$$\frac{\partial^2 p}{\partial r^2} + \frac{1}{r}\frac{\partial p}{\partial r} = \frac{\phi \mu c}{k}\frac{\partial p}{\partial t} \tag{2.1}$$

where p represents the pressure, r the reservoir radius, ϕ the porosity, μ the viscosity, c the compressibility k the permeability and t the time.

The equation is an essential part of the current work and will be expanded for the purpose of describing the stress sensitive reservoir.

Dimensionless variables

Using dimensionless variables are basically a means to ease calculations, as consideration of units does not need to be considered. All dimensionless variables are put together corresponding real ones, to make the functions dimensionless.

As an illustration the dimensionless diffusivity equation for radial flow is given by

$$\frac{\partial^2 p_D}{\partial {r_D}^2} + \frac{1}{r_D}\frac{\partial p_D}{\partial r_D} = \frac{\partial p_D}{\partial t_D} \tag{2.2}$$

where index D represents the dimensionless form of variables.

2.3 Types of Well Tests

The types of well tests used to investigate the new developed solution for stress-sensitive reservoirs include drawdown and buildup tests as well as two other typical tests curves that are described below.

2.3.1 Interference Test

An interference test involves two or more wells and is performed by producing or injecting from one well and monitoring the pressure response from another or several others. The objective is to investigate if pressure communication between the two wells are present and, if communication exists, finding estimates of the permeability, k, and storage capacity, ϕc_t, Lee (1982). If more observation wells then one is present one can also investigate directional permeability.

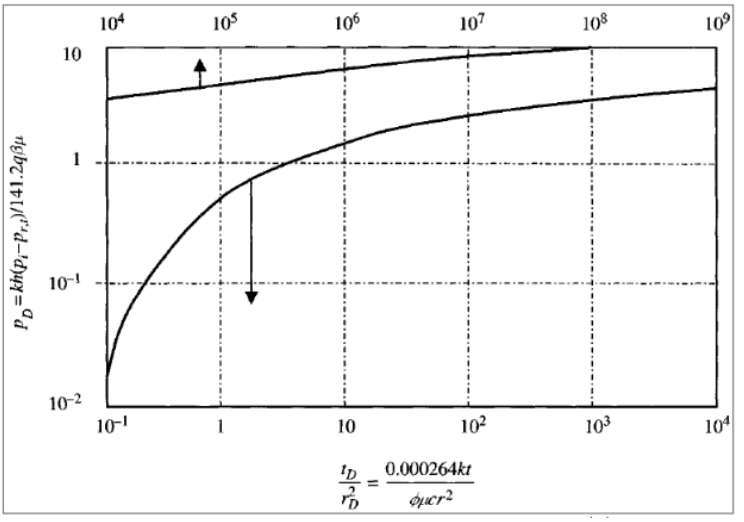

Figure 2.3: Interference test type curve, Earlougher (1977).

In a simplified model with one producing and one observation well, the wells are assumed to be a distance r between each other. The producing well starts to produce at time 0 and after some time the pressure response is felt in the observation well. The pressure in the

producing well will consequently start decreasing. The magnitude and amount of time of the two differing pressure responses gives information about the reservoir properties close to the two wells, Lee (1982).

The interference test is usually plotted by type curve analysis. A typical type curve for a homogeneous reservoir is represented in figure 2.3.

For two or more wells spaced close together, a situation that might be encountered with horizontal wells, the interference test can also be used to find the equivalent wellbore radius r_{we}. The equivalent wellbore radius may be used to represent a skin zone when including skin in its normal form is not convenient, Jelmert (2013). Including skin in some situations might give an unrealistic pressure jump, whereas the equivalent radius represents the same phenomena by a mathematical identity which is often useful. For a damaged well the equivalent radius is less than the radius of the wellbore, whereas for a stimulated well the equivalent radius is larger than that of the well. The relationship between the equivalent wellbore radius, r_{ew}, and the wellbore radius, r_w , can be given as follows

$$r_{we} = r_w e^S \tag{2.3}$$

where S is the skin factor.

2.3.2 Horner Analysis

The pressure build up analysis describes the pressure buildup behavior after the well has been shut in. It is a useful tool in reservoir engineering to determine the reservoir behavior, as the pressure build up usually follows a defined trend.

The analytical solution for the build up pressure is usually found by superposition in time. The superposition solution is based on the drawdown solution and assumes one or more fictitious wells to replace the actual well and its location. The buildup solution is consequently the pressure sum of the fictitious well/wells and the actual well, Jelmert (2013).

The buildup pressure response is typically analyzed by a Horner type graph. This is a semilog plot of the well shut in pressure, p_{ws} versus the Horner time, $\frac{t_p+\Delta t}{\Delta t}$, as illustrated in 2.4. Where t_p is the flowing time before shut in and Δt is the shut in time. The straight

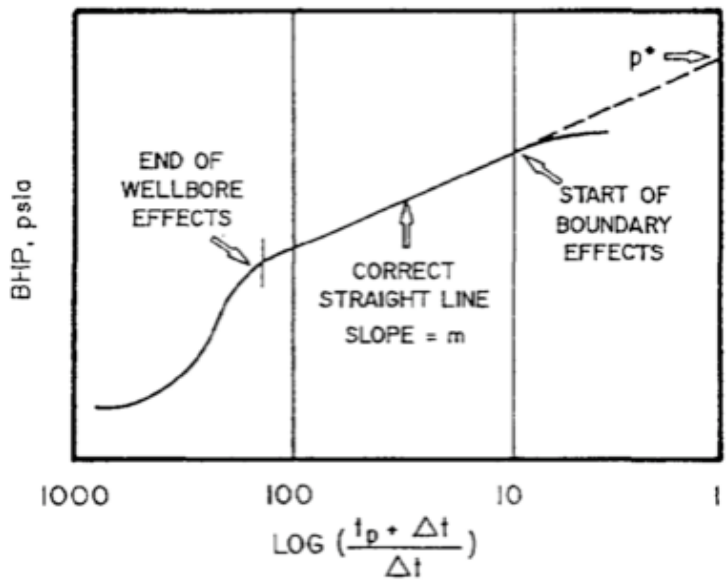

Figure 2.4: Typical Horner graph illustrating different behaviors with pressure and Horner time, Matthews and Russell (1967).

line part of the curve can be used to find the permeability and skin from the slope of the straight line, m, as seen in figure 2.4

2.4 Wellbore Storage and Skin

Storage and skin are two main effects that may cause pressure changes near the wellbore.

The wellbore storage describes the wellbores capacity to store fluid. As pressure increases more fluid is stored. Wellbore storage is basically a nuisance effect, affecting the form of pressure transients, which must be recognized in order to make an accurate analysis of the well flow, Grant and Bixley (2011). The effect of wellbore storage on the transient response can be seen in figure 2.5, showing the homogeneous reservoir solution including dimensionless storage, C_D and skin, S. From the early time unit slope the wellbore storage coefficient, C, can be found.

It is not unusual for the permeability near the wellbore to be reduced compared to that of the reservoir. Mud filtrate, cement slurry or clay particles that enter the formation during

well operations may cause this alteration and the region is thereby called the skin zone, Ahmed (2001). In reservoir engineering the effect of skin is calculated as an additional local pressure drop, Δp_{skin}. A positive value indicates an additional pressure drop and hence a smaller permeability in this zone, whilst a negative skin indicates a stimulated well which will require less pressure drawdown to produce at same rate, q, and zero skin means that there is no reduction to the near wellbore permeability.

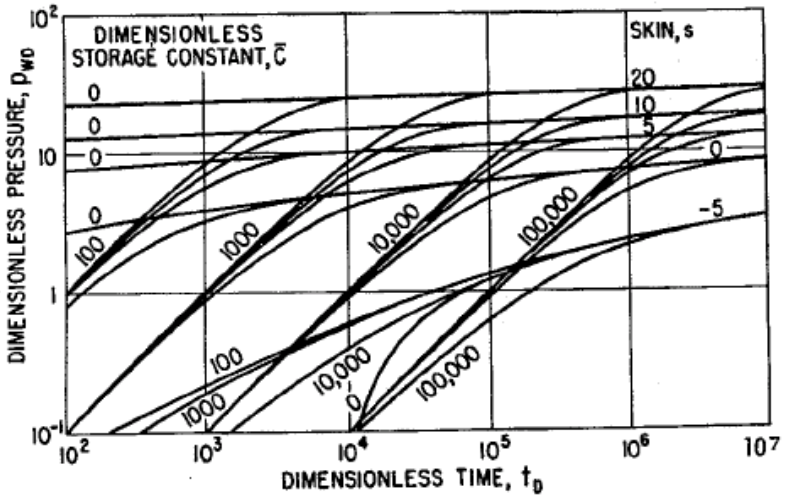

Figure 2.5: Typical curves for different values of wellbore storage and skin, Lee (1982).

Chapter 3

Literature Review

The present chapter represents relevant literature on the stress-sensitive reservoir and includes modified paragraphs from the semester project, Lillehammer (2014).

3.1 The Stress-Sensitive Reservoir

Stress-sensitivity investigates the performance of reservoirs under the extortion of effective stresses which changes the parameters of physical properties in the rock, Renpu (2011). Reservoir depletion and subsequent subsidence as a cause of pressure decrease cause the effective stress on the matrix to increase leading to the change in reservoir properties. Reservoirs with such behavior are often described as unconventional.

3.2 Unconventional Reservoirs

An unconventional reservoir is by definition *"fossil fuels found in a geological setting, differing from that of conventional deposits of oil or gas, and requiring specific technology to develop"*, Cutler J. Morris (2009). Unconventional reservoirs have low permeability and porosity, making them more difficult to produce. However *"Only a third of worldwide oil and gas reserves are conventional..."*, from Geoscience (2015), meaning that unconventional reservoirs play an important role in the petroleum industry.

In the U.S. the extraction of gas from shale formations has been performed for more than a

decade. In later years new technology has enabled petroleum companies to develop these resources more economically and both the interest for unconventional resources as well as the development of such fields have grown significantly, from Geoscience (2015).

3.3 Compaction Due to Stress

In a hydrocarbon bearing formation there will be pressurized fluid in a solid framework. Both the fluid and the solid support stresses on the material, Doornhof et al. (2006). This is a concept described as the effective-stress principle stating that "*the stress affecting the behavior of a solid material is the applied stress minus the support from the pore-fluid pressure*"Doornhof et al. (2006). As production of fluids from a reservoir starts the pore pressure decreases and consequently increases the vertical effective stresses acting on the solid matrix. This phenomenon of changing stress situation in the formation results in compaction. The degree of compaction depends on the rock properties and boundary conditions of the formation.

3.4 Pressure Dependent Variables

From laboratory studies and observed pressure behavior in wells it is known that properties like porosity and permeability decrease as the reservoir is depleted and the pressure declines. Depletion causes the effective overburden pressure to increase which again leads to deformation, compression and closure of rock pores, Ren and Guo (2014). It is found that flow rates in stress-sensitive reservoirs may be much lower than the production predicted by the use of equations with constant rock properties.

There are many studies on pressure dependent variables, especially on the pressure dependency of permeability. The decrease in permeability is by many believed to be the primary cause for early pressure decline and is consequently the main focus of research. There are two main approaches for incorporating the pressure dependency into models. These are the pseudo pressure approach and the permeability-stress function approach, Ren and Guo (2014).

Hussainy et al. (1966) proposed a quasi-linear flow equation with a pressure dependent diffusivity term as early as in 1966. The equation was reduced, by the use of a pseudo-pressure, to a form similar to the diffusivity equation. This was an industry improvement

for describing the flow of real gas through porous media. Earlier approximations were only applicable for small pressure changes, which was not the case for stress-sensitive reservoirs.

Vairogs et al. (1971) found that the reduction of permeability in tight gas reservoirs had a significant effect on the production. The permeability was expressed as a function of stress, which again is a function of pore pressure. By the use of numerical modelling they found indications that the flow rate as a function of wellbore pressure was decreasing when considering permeability varying with stress.

Many analytical solutions on the basis of what Hussainy et al. (1966) found have later developed. Chien and Caudle (1994) proposed a new gas potential where pressure dependent variables such as viscosity, compressibility, porosity and permeability for gas reservoirs were considered. A diffusivity equation for real gas flow with non-constant diffusivity term and pressure dependent properties was derived from the continuity equation.

Economides et al. (1994) proposed a step-pressure test to evaluate stress sensitivity of reservoir permeability where the pseudo-pressure was modified to include the pressure dependent permeability. The proposed method was valid both for oil and gas flow.

Sun and Branch (2007) studied the effect of productivity and performance for the stress-sensitive gas reservoir. Utilizing a pseudo pressure function and assuming no-Darcy turbulent flow they expressed the material balance equation for an overpressured gas reservoir. They included a permeability modulus found by expressing the permeability as an exponential function of pressure.

Chen and Li (2008) and jiao Xiao et al. (2009) among others also included the assumption of an exponential pressure-permeability reduction. Kikani and Pedrosa (1991) proposed an approach to define stress-dependent permeability by defining a permeability modulus, γ, similar to that defined for different types of compressibility.

$$\gamma = \left(\frac{1}{k}\right)\frac{\partial k}{\partial p} \tag{3.1}$$

The pressure dependent permeability can by 3.1 be expressed exponentially as,

$$k = k_{ref}e^{-\gamma(p-p_{ref})} \tag{3.2}$$

where k_{ref} and p_{ref} are the initial reference values. Equation 3.2 was based on findings

done by Wyble (1958), who investigated the property change of cores when moved from the ground to the laboratory. This description of pressure dependent permeability is also referred to as the one-parameter exponential function.

The permeability can also be described as stepwise model, presented in the work of both Zhang and Ambastha (1994) and Ambastha and Zhang (1996). This representation takes into consideration that the permeability changes with changing net confining pressure. It has not been widely used in the industry, as the critical pressure is difficult to determine accurate.

Other models include the two-parameter exponential function also represented by Ambastha and Zhang (1996), as well as the power function model used by Ren and Guo (2014).

This study will only consider the one-parameter exponential model of permeability and also assume that this model can give a fair representation of other pressure dependent parameters such as viscosity, density and porosity/thickness. Describing permeability, and also porosity, as a one-parameter exponential function is accepted as a good approximation by several studies, Kikani and Pedrosa (1991). Including pressure dependencies of other parameters is not as widely done.

A study assuming pressure dependency of permeability and porosity but also reservoir thickness and viscosity is represented by Finjord and Aadnoy (1989). The article states that the variation in height as a function of pressure corresponds to letting the bulk volume vary with pressure. Jelmert (2014) represented a solution to the inflow performance relationship by considering pressure variation in permeability, viscosity and fluid density.

Jelmert (2014) described the permeability but also the viscosity and fluid density by the same exponential relation as equation 3.2, these were put together to one composite elastic modulus. In the semester project of Lillehammer (2014) the same relationships were used, and also included the exponential relationship of thickness.

3.5 Transient Solutions

Several transient solutions to the diffusivity equation with stress-sensitivity have been represented in literature. Analytical approximations, numerical models or iterative solutions represent the transient flow response.

The study of R.Raghavan et al. (1972) introduced a pseudo-pressure function on stress sensitivity which corresponds to the conventional equations of Everdingen and Hurst (1949). The pseudo-pressure approach has some disadvantage in that the rock and fluid properties versus pressure need to be known prior to each pressure level. The diffusivity equation found by this approach also has a nonlinear term, which usually is approached by evaluating the pressure at initial values to make the problem tractable, Zhang (1994).

The approach of a permeability-stress function considering the pressure dependency of permeability has been widely used in combination with pressure transient behavior. Pedrosa (1986) obtained a analytical solution for the pressure transient response by solving the radial flow equation analytically with pressure dependent properties, taking into account the reduction in permeability caused by increase in effective stress. The solution is a first order approximation for a line-source well producing at constant rate from an infinite radial reservoir found by the use of perturbation.

Kikani and Pedrosa (1991) further developed the model, presenting also the second order analytical perturbation solution as well as a zero-order solution including wellbore storage and skin, to investigate the effects of these phenomenon's on a stress-sensitive formation. The work of both Pedrosa (1986) and Kikani and Pedrosa (1991) forms much of the basis for the work of this report and an extended description of their work is included in chapter 4.

Zhang and Ambastha (1994) suggested a numerical solution to study pressure transient response. Another analytical approximation was suggested by Jelmert and Selseng (1998) who introduced normalized permeability variables to linearize the diffusivity equation. The solution was found to match well with Kikani and Pedrosa (1991) second order perturbation technique.

Liehui et al. (2010) presented a analytical well test model by the concept of exponential one parameter permeability modulus and non-uniform height. The effect of storage and skin was also included. The model was found analytically in Laplace space and inverted to time domain by the use of Stehfest algorithm, see section 4.1.3.3. The authors found that the stress-sensitivity had little effect on the wellbore storage periode and started to deviate from the homogeneous solution at intermediate to late times.

Kohlhaas and Miller (1969) represented a transient solution with pressure dependency of permeability, porosity and thickness. The solution was transformed to obtain the form of the diffusivity equation by the use of a transformation variable. Kohlhaas and Miller (1969) represented a solution for vertical flow in a horizontal layer and used this to find

the degree of shrinkage of the layer as a function of time. The shrinkage is represented as an integral from zero to layer thickness in the z-direction. By assuming that the thickness is constant they represented an equation for the ultimate shrinkage as a function of bulk volume compressibility, layer thickness, density and the change in fluid head. For typical data Kohlhaas and Miller (1969) found that the maximum amount of shrinkage was around 0.1"%" of the total thickness for a pressure drop of 1000 psi.

Chapter 4

Relevant Mathematical Theory

To develop a new solution for the pressure transient response of a stress sensitive reservoir the work of Pedrosa (1986) and Kikani and Pedrosa (1991) is studied. Their work, together with mathematical theory represented in this chapter, forms the basis for further development.

This chapter will first represent Kikani and Pedrosa's analytical solution, before going into detail on different results depending on the accuracy of the solution method used.

4.1 Analytical Solution of the Stress-Sensitive Diffusivity Equation

Kikani and Pedrosa based their model on the the permeability modulus expressed as a function of varying pressure, equation 4.1, and the continuity equation , equation 4.2.

$$\gamma = \frac{1}{k}\frac{dk}{dp} \tag{4.1}$$

The diffusivity equation for single-phase liquid in an isotropic and homogeneous reservoir with slightly compressible fluid and using Darcy's law is expressed as

$$\frac{1}{r}\frac{\partial}{\partial r}\left(r\rho\frac{\partial p}{\partial r}\right) = \frac{\partial(\phi\rho)}{\partial t} \tag{4.2}$$

where r represents the reservoir radius, ϕ the porosity and ρ the density.

In terms of a stress-sensitivity Kikani and Pedrosa (1991) expanded the equation

$$\frac{\partial^2 p}{\partial r^2} + \frac{1}{r}\frac{\partial p}{\partial r} + (c_l + \gamma)\left(\frac{\partial p}{\partial r}\right)^2 = \frac{\phi\mu}{k}(c_l + c_m)\frac{\partial p}{\partial t} \tag{4.3}$$

where c_l represents the liquid compressibility and c_m the matrix compressibility.

The equation is strongly nonlinear because of the pressure gradient square term and the permeability gradient. A common assumption is that the pressure gradient term is small. This is not valid for a stress sensitive reservoir as the pressure gradients near the wellbore are usually very high. The permeability modulus is also not small enough to be neglected, Kikani and Pedrosa (1991).

By assuming constant moduli of compressibility and permeability and evaluating the diffusivity at the initial pressure the equation was further linearized. Details of these calculations are not presented here, but a similar procedure is presented for the development of the new solution in chapter 5.

Kikani and Pedrosa (1991) introduced dimensionless variables so that the equation simplifies to

$$\frac{\partial^2 p_D}{\partial {r^2}_D} + \frac{1}{r_D}\frac{\partial p_D}{\partial r_D} + (\gamma_D)\left(\frac{\partial p_D}{\partial r_D}\right)^2 = e^{\gamma_D p_D}\frac{\partial p_D}{\partial t_D} \tag{4.4}$$

Here γ_D defines the dimensionless permeability modulus.

Equation 4.4 is not convenient to solve analytically so Pedrosa (1986) introduced the following new dimensionless dependent variable, η, which is related to the dimensionless pressure according to

$$p_D(r_D, t_D) = -\frac{1}{\gamma_D}\ln\left[1 - \gamma_D \eta(r_D, t_D)\right] \tag{4.5}$$

The zero-order approximation of this solution was found to be

$$\eta_o = \frac{1}{2}E_i\left(\frac{{r_D}^2}{4t_D}\right) \tag{4.6}$$

where E_i is the exponential integral function, explained in section 4.1.1

The dimensionless pressure for the zero order solution is thereby given as as

$$p_D = -\frac{1}{\gamma_D}\ln(1-\gamma_D\frac{1}{2}E_i\left(\frac{{r_D}^2}{4t_D}\right) \tag{4.7}$$

The first order approximation was found as

$$\eta_1 = \frac{1}{2}E_i(2z) - \frac{1}{4}\left(1-e^{-z}\right)E_i(z) \tag{4.8}$$

where z is equal to ${r_D}^2/4t_D$ and the index of η represents the order of approximation.

Kikani and Pedrosa (1991) also represented a second order solution, which is not included in this text. The different orders of solutions are found by the use of perturbation. This is a method of calculations where a system of equations is divided into a part that is exactly calculable and a small term, which prevents the whole system from being exactly calculable, Daintith (2010). The higher the order, the more accuracy will be achieved. Kikani and Pedrosa found that the second order solution could be neglected and also that the zero order solution was adequate for most purposes.

To obtain the buildup solution superposition was applied to each order of perturbation solution. No direct superposition of the governing equation 4.4 can be found as this equation is non linear, Kikani and Pedrosa (1991). The zero order buildup solution was represented by Pedrosa (1986) as

$$\eta_o = \frac{1}{2}E_i\left(\frac{{r_D}^2}{4(t_{pD}+\Delta t_D)}\right) - \frac{1}{2}E_i\left(\frac{{r_D}^2}{4\Delta t_D}\right) \tag{4.9}$$

The dimensionless pressure can then by equation 4.5 be expressed as

$$p_D = -\frac{1}{\gamma_D}\ln\left\{1-\frac{\gamma_D}{2}E_i\left[\frac{{r_D}^2}{4(t_{pD}+\Delta t_D)}\right] + \frac{\gamma_D}{2}E_i\left(\frac{{r_D}^2}{4\Delta t_D}\right)\right\} \tag{4.10}$$

Solution and graphical representation of the behavior of the dimensionless pressure for drawdown, equation 4.7 and buildup, equation 4.10 can be achieved by different approaches represented below.

4.1.1 Exponential Integral Function

The dimensionless drawdown and buildup pressures can be found directly from 4.7 and 4.10, by solving the exponential integral functions. MATLAB has a built-in E_i function, $ei(x)$, which returns the one-argument exponential integral, Mathworks (2015), defined as

$$ei(x) = \int_x^\infty \frac{e^{-t}}{t} dt \tag{4.11}$$

4.1.2 Logarithmic Approximation

For values of the argument of the exponential integral function less than 0.01 the logarithmic approximation to the E_i function and thus the drawdown and buildup solution respectively, simplifies to

$$p_D = -\frac{1}{\gamma_D} \ln\left[1 - \frac{\gamma_D}{2} \ln t_D\right] \tag{4.12}$$

$$p_D = -\frac{1}{\gamma_D} \ln\left[1 - \frac{\gamma_D}{2} \ln \frac{t_{pD} + \Delta t_D}{\Delta t_D}\right] \tag{4.13}$$

Disregarding any values that are not within the desired limit, means less accuracy to the solution. At the same time the solution is easy to implement by the use of any computing program, like Excel or MATLAB. These solutions were therefor used to confirm that the extended solutions followed the same behavior.

4.1.3 Laplace Transform Solution

Equations 4.7 and 4.10 can also be written in terms of the dimensionless pressure functions

For drawdown

$$p_D = -\frac{1}{\gamma_D} \ln\left[1 - \frac{\gamma_D}{2} p_D(t_D)\right] \tag{4.14}$$

For buildup

$$p_D = -\frac{1}{\gamma_D} \ln \left[1 - \frac{\gamma_D}{2} p_D(t_{pD} + \Delta t_D) + \frac{\gamma_D}{2} p_D(\Delta t_D) \right] \tag{4.15}$$

where the dimensionless pressure terms can be found by Laplace transformation.

4.1.3.1 Laplace Space Solution

The Laplace transform is an integral transform for solving physical problems, Wolfram-Mathworld (2015). It is a means of easing complicated equations by shifting the equation from time domain to what is called Laplace space. The integral transform can be represented as

$$L_t \left[f(t) \right] (s) = \int_0^\infty f(t) e^{-st} dt \tag{4.16}$$

Where f (t) is a function defined for all values of the real variable t, L is the Laplace operator and s is some space parameter.

Complex equations are usually easier to solve in Laplace space for example by the use of modified Bessel functions. When the equation is solved in Laplace space it can be inverted back to time domain to obtain the final result. An overview of the process is illustrated in figure 4.1.

The pressure functions in equations 4.14 and 4.15 can be inverted to Laplace space by the use of the integral transform, 4.16.

4.1.3.2 Line Source Solution in Laplace Space with the Use of Modified Bessel Functions

A well-known solution to the diffusivity equation is the line source solution. This solution has some simplifying assumptions that make it easier to handle. The solution is represented in the text as it forms the basis for understanding the Laplace solutions that are represented by Kikani and Pedrosa (1991) and for the new solution. The line source solution is also used to investigate how a stress-sensitive solution deviates from a homogeneous solution.

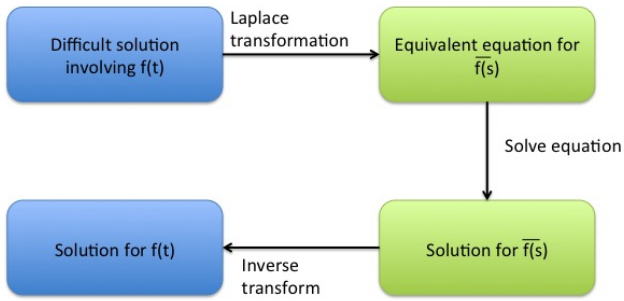

Figure 4.1: Laplace transformation work-flow showing how to inverse a difficult equation in time domain to Laplace space. The equation will usually be easier to solve in Laplace space, and then need to be inversed back to time domain to get the final solution, this last step is often the hardest.

The simplifying assumptions for the line source solution are, Stewart (2011)

- Constant flow rate, q, for $t \geq 0$
- Infinite acting reservoir $p_D(t_D) \rightarrow 0$ for $r_D \rightarrow \infty$
- Well shaped like a line
- Well is fully penetrated

The governing equation in time domain for the line source solution in dimensionless form is given by

$$\frac{\partial^2 p_D}{\partial {r_D}^2} + \frac{1}{r_D}\frac{\partial p_D}{\partial r_D} = \frac{\partial p_D}{\partial t_D} \tag{4.17}$$

Expressed in Laplace space

$$\frac{\partial^2 \overline{p}_D(s)}{\partial {r_D}^2} + \frac{1}{r_D}\frac{\partial \overline{p}_D(s)}{\partial r_D} = s\overline{p}_D(s) + p_D(0) \tag{4.18}$$

The last term of equation 4.18 on the left side is zero, found for the initial condition, $t_D = 0$, Stewart (2011).

The solution of equation 4.18 has the form of the modified Bessel equation of zero order

$$x^2 \frac{dy}{dx^2} + x\frac{dy}{dx} - x^2 y = 0 \tag{4.19}$$

with the following solution,

$$\overline{p}_D = AI_0(x) + BK_0(x) \tag{4.20}$$

where I_0 and K_0 are modified Bessel functions of first and second kind with order of zero. Modified Bessel equations are infinite series,

$$I_0(x) = 1 + \frac{\frac{1}{4}x^2}{(1!)^2} + \frac{\left(\frac{1}{4}x^2\right)^2}{(2!)^2} + \frac{\left(\frac{1}{4}x^3\right)^3}{(3!)^2}..... \tag{4.21}$$

that can be time consuming to solve, and polynomial approximations usually gives sufficient accuracy, Jelmert (Fall 2014).

The modified Bessel functions can also be solved by built-in MATLAB functions, *I = besseli(nu,Z)* and *K = besselk(nu,Z)*. Where *nu* defines the order, which in this case is zero, and *Z* defines the variable, for this case $r_D\sqrt{s}$.

From 4.20 the following modified Bessel equation expresses the line source solution

$$\overline{p}_D = AI_0\left(r_D\sqrt{s}\right) + BK_0\left(r_D\sqrt{s}\right) \tag{4.22}$$

where A and B are constants to be determined.

From the outer boundary conditions

$$\overline{p}_D = 0 \Leftrightarrow r_D \to \infty \tag{4.23}$$

which again leads to

$$A = 0 \to I_0 = 0 \tag{4.24}$$

so that the dimensionless pressure in Laplace space is

$$\overline{p}_D = BK_0\left(r_D\sqrt{s}\right) \tag{4.25}$$

Taking the derivative of 4.25 with respect to the dimensionless distance and by multiplying both sides with r_D

$$r_D\frac{d\overline{p}_D}{dr_D} = -Br_D\sqrt{s}K_1\left(r_D\sqrt{s}\right) \tag{4.26}$$

From the inner boundary condition

$$\lim_{r_D\to 0} = \left(r_D\frac{\partial p_D}{\partial r_D}\right) = -1u(t) \tag{4.27}$$

where the term on the left side, u (t), is called the heavy side unit step function. In Laplace space this function corresponds to $\frac{1}{s}$

$$\lim_{r_D\to 0}\left(-Br_D\sqrt{s}K_1\left(r_D\sqrt{s}\right)\right) = -\frac{1}{s} \tag{4.28}$$

The modified Bessel functions have limiting forms for small arguments, where $K_1(x) = -\frac{1}{x}$ so that

$$K_1\left(r_D\sqrt{s}\right) \to \frac{1}{r_D\sqrt{s}} \text{ when } r_D \to 0 \tag{4.29}$$

which again means that

$$B = \frac{1}{s} \tag{4.30}$$

Substituting this back to equation 4.25 the Laplace solution is obtained

$$\overline{p}_D = \frac{1}{s}K_0\left(r_D\sqrt{s}\right) \tag{4.31}$$

At the wellbore, where $r_D = 1$

$$\overline{p}_{wD} = \frac{1}{s} K_0\left(\sqrt{s}\right) \tag{4.32}$$

To obtain the time domain solution inverse transformation of equation 4.31 needs to be performed. This can be obtained by use of transform tables. For more complicated Laplace solutions, as the one presented by Kikani and Pedrosa (1991) where skin and storage is included

$$\overline{p}_{wD} = \frac{K_0\left(\sqrt{s}\right) + S\sqrt{s}K_1\left(\sqrt{s}\right)}{s\left(\sqrt{s}K_1\left(\sqrt{s}\right) + C_D s\left[K_0\left(\sqrt{s}\right) + S\sqrt{s}K_1\left(\sqrt{s}\right)\right]\right)} \tag{4.33}$$

it is not possible to obtain an exact inverse transformation. The use of numerical approximation as Stefhest algorithm is then utilized.

4.1.3.3 Gaver-Stehfest Algorithm

Well testing problems are often inverted and solved in the Laplace space to ease calculations. When equations become complex they may also be impossible or difficult to invert back to the time solution. Such problems have to be solved by the use of numerical analysis, like the Stehfest algorithm, Jelmert (Fall 2014). If the Laplace space solution f(s) is given the time domain solution f(t) may be found approximately at a specific time point t=T.

$$P_a(T) = \frac{\ln 2}{T} \sum_{i=1}^{N} V_i \overline{p}(s)_{s=i\frac{\ln 2}{T}} \tag{4.34}$$

where N is an integer also called the Stehfest number and V_i is a set of predetermined coefficients that are dependent of N.

The coefficients are calculated from the following formula

$$V_i = (-1)^{N/2+i} + \sum_{K=M}^{L} \frac{k^{N/2}(2k)!}{\left(\frac{N}{2}-k\right)!k!(k-1)!(i-k)!(2k-i)!} \tag{4.35}$$

where

$$L = \min\left[i, \frac{N}{2}\right] \tag{4.36}$$

$$M = \frac{i+1}{2} \tag{4.37}$$

The Stehfest number, N, should be even. Theoretically the approximation becomes better with a larger value of N, Jelmert (Fall 2014). In practice the round off errors will worsen if N is set too large. Stehfest used N=10 for 8 digit arithmetic and N=18 with double precision arithmetic.

When the Stehfest algorithm is used to generate the dimensionless pressure solution $P_D(t)$ from its Laplace transform $P_D(s)$, it is computed at preselected values of t_D sufficient to cover the range of interest.

An implementation routine for the Stehfest algorithm is readily available form MATLAB sites, Srigutomo (2014). The MATLAB code is also included in Appendix B.

4.1.3.4 Well With Storage and Skin

What makes the Laplace solution desirable and some of the reason it is included in the present work is that it is a convenient way to express solutions including wellbore storage and skin effects, as shown in 4.33, found by Kikani and Pedrosa (1991). For given values of C_D and S this can be inverted back to time domain using the Stehfest algorithm for a range of values of t_D

The line source solution including storage and skin can be found by equation 4.33 by noting that as *s* becomes smaller the product $[\sqrt{s}K_1(\sqrt{s})]$ approaches unity, Agarwal et al. (1970). The resulting equation with C_D and S becomes

$$\frac{K_0\left(\sqrt{s}\right) + S}{s\left[1 + C_D s K_0\left(\sqrt{s}\right) + S C_D s\right]} \tag{4.38}$$

4.2 Verification of Model

The solutions represented in the above sections, were implemented into MATLAB for verification on a Horner type curve, as illustrated in 4.2. The logarithmic approximation, sec-

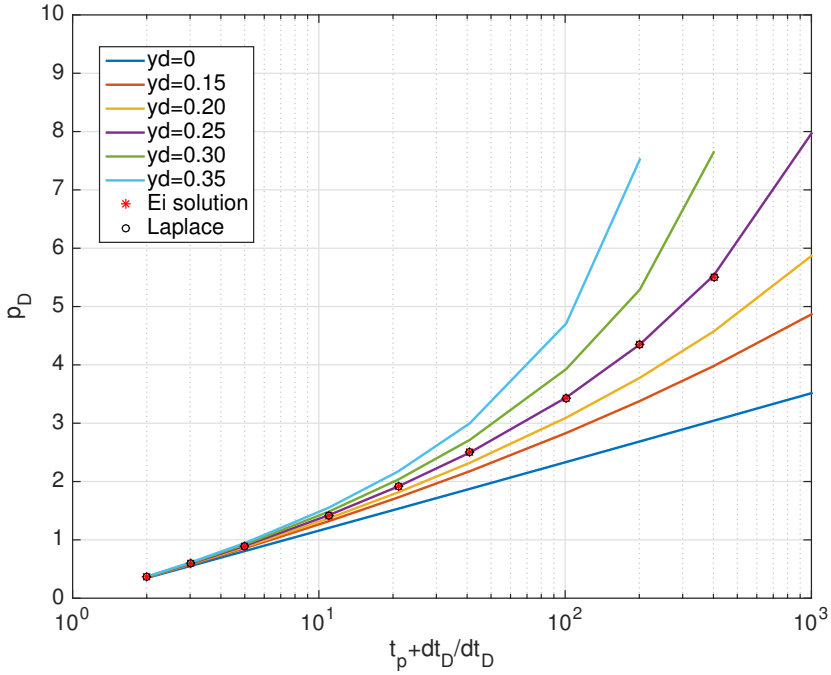

Figure 4.2: Horner type curve showing Kikani and Pedrosa (1991) zero order solutions for different values of γ_D, compared to the E_i solution and Laplace solution for $\gamma_D = 0.25$

tion 4.1.2, was plotted for γ_D values ranging from 0 to 0.35. The direct E_i solution, section 4.1.1, and the Laplace space solution, section 4.1.3.1 was plotted for $\gamma_D = 0.25$.

The resulting curves in figure 4.2 matches those found by Kikani and Pedrosa (1991) and gives confidence to further develop the model.

Chapter 5

New Analytical Solution

The solution represented below is derived based on extensive research of the mathematical theory represented in chapter 4.

The semester project, Lillehammer (2014), concluded that *"The reservoir properties of permeability, porosity, viscosity, density, compressibility and thickness can all be estimated as exponential functions of pressure, and they correlate well within the accepted error margin."* The same assumptions are used in the current derivations. The elasticity modulus, which includes all the pressure dependent parameter values, is included in the diffusivity equation by the use of the transmissivity modulus. This means a new solution to the diffusivity equation has to be derived, with boundary values for the present problem.

5.1 Deriving Basic Relationships Based on Elastic Moduli

The pressure dependent variables permeability, density, viscosity and thickness are all represented by exponential equations, Lillehammer (2014), found by plotting the known values and performing exponential regression. The relationship between compressibility, formation volume factor, B, and density can be given as

$$c = B\frac{dB^{-1}}{dp} = \frac{1}{\rho}\frac{d\rho}{dp} \tag{5.1}$$

This results in four exponential expressions, with their corresponding moduli. All moduli are assumed constant.

$$\rho = \rho_i e^{c(p_i - p)} \tag{5.2a}$$

$$\mu = \mu_i e^{\upsilon(p_i - p)} \tag{5.2b}$$

$$k = k_i e^{\gamma(p_i - p)} \tag{5.2c}$$

$$h = h_i \frac{1 - \phi_i}{1 - \phi_i e^{\alpha \Delta p}} = h = h_i e^{\xi(p_i - p)} \tag{5.2d}$$

Here c , υ, γ and ξ denotes the constant elasticity modulus for each variable respectively,(details included in Appendix A).

The combined moduli, τ, can thereby be expressed by,

$$\tau = \gamma + c + \xi - \upsilon \tag{5.3}$$

The transmissivity, T(p) may be defined as

$$T(p) = \frac{k(p)h(p)\rho(p)}{\mu(p)} \tag{5.4}$$

where T(p) is related to the normalized transmissivity, $T_n(p)$, and the initial transmissivity, T_i, as follows

$$T(p) = T_n(p)T_i \tag{5.5}$$

By this relationship T(p) can equally be expressed as

$$T(p) = \frac{k(p_i)h(p_i)\rho(p_i)}{\mu(p_i)} T_n(p) \tag{5.6}$$

The change in transmissivity can consequently be expressed as

$$\Delta T(p) = T_i - T(p) \tag{5.7}$$

and then equally for the normalized transmissivity, remembering the relationship given in equation 5.5

$$\Delta T_n(p) = 1 - T_n(p) \tag{5.8}$$

The elasticity modulus can moreover be expressed in terms of transmissibility

$$\tau = \gamma + c + \xi - \upsilon = \frac{1}{T_n}\frac{dT_n}{dp} = \frac{1}{T_n}\frac{d\Delta T_n}{d\Delta p} \tag{5.9}$$

Integrating T_n in equation 5.9 by assuming that the moduli τ results in T_n as an exponential function of pressure.

$$T_n = 1 + \Delta T_n = e^{-\tau(p - p_{ref})} \tag{5.10}$$

Where p is a pressure to be found, in this report the wellbore pressure, and p_{ref} is the pressure at some boundary, in this report the initial pressure.

Further details of these calculations can be found in Appendix A.

5.2 Including the Transmissivity into New Formulation by Use of Raghavan Solution

R.Raghavan et al. (1972) obtained the following relationship for the diffusivity equation with pressure dependent variables, R.Raghavan et al. (1972)(equation 10).

$$\frac{1}{r}\frac{\partial}{\partial r}\left(\frac{k(p)h(p)\rho(p)}{\mu(p)} r \frac{\partial \Delta p}{\partial r}\right) = h(p)\rho(p)\varphi(p)\left[c_1 + c_f(p)\right]\frac{\partial \Delta p}{\partial t} \tag{5.11}$$

where c_f is the formation compressibility and c_1 the initial compressibility.

By the use of the relationship of transmissivities 5.5 this can equivalently be written as

$$\frac{1}{r}\frac{\partial}{\partial r}\left(\frac{k_i h_i \rho_i}{\mu_i}\frac{k_n(p)h_n\rho_n(p)}{\mu_n(p)}r\frac{\partial \Delta p}{\partial r}\right) = h(p)\rho(p)\varphi(p)\left[c_1 + c_f(p)\right]\frac{\partial \Delta p}{\partial t} \tag{5.12}$$

Next, moving the initial terms to the right hand side and by including the expression for the dimensionless radius

$$r_D = \frac{r}{r_w} \tag{5.13}$$

$$\frac{1}{r_D}\frac{\partial}{\partial r_D}\left(T_n(p)r_D\frac{\partial \Delta p}{\partial r_D}\right) = \frac{{r_w}^2\mu_i}{k_i h_i \rho_i}h(p)\rho(p)\varphi(p)\left[c_1 + c_f(p)\right]\frac{\partial \Delta p}{\partial t} \tag{5.14}$$

Then noting that $\frac{h(p)}{h_i}$ and $\frac{\rho(p)}{\rho_i}$ can be replaced by h_n and ρ_n the right hand side simplifies slightly

$$\frac{1}{r_D}\frac{\partial}{\partial r_D}\left(T_n(p)r_D\frac{\partial \Delta p}{\partial r_D}\right) = \frac{{r_w}^2\mu_i}{k_i}h_n(p)\rho_n(p)\varphi(p)\left[c_1 + c_f(p)\right]\frac{\partial \Delta p}{\partial t} \tag{5.15}$$

Equation 5.15 is strongly non-linear because of the pressure dependent terms. The normal way to linearize such an equation is by evaluating it at the initial pressure. This will cancel out the pressure dependent terms on the right hand side.

$$\frac{1}{r_D}\frac{\partial}{\partial r_D}\left(T_n(p)r_D\frac{\partial \Delta p}{\partial r_D}\right) = \frac{{r_w}^2\mu_i}{k_i}1\cdot 1\cdot\varphi_i c_{ti}\frac{\partial \Delta p}{\partial t} \tag{5.16}$$

Noting that the expression for the compressibilities on the right hand side at initial condition is the initial total compressibility the dimensionless time relationship is found, expressed as

$$t_D = \frac{k_i t}{\varphi_i \mu_i c_{ti} {r_w}^2} \tag{5.17}$$

This makes it possible to express the equation in terms of dimensionless variables

$$\frac{1}{r_D}\frac{\partial}{\partial r_D}\left(T_n(p)r_D\frac{\partial \Delta p}{\partial r_D}\right) = \frac{\partial \Delta p}{\partial t_D} \tag{5.18}$$

and by dimensionless pressure which is given as

$$p_D = \alpha \Delta p \tag{5.19}$$

So that the equation reduces to

$$\frac{1}{r_D}\frac{\partial}{\partial r}_D \left(T_n(p) r_D \frac{\partial p_D}{\partial r_D} \right) = \frac{\partial p_D}{\partial t_D} \tag{5.20}$$

To further solve this equation it needs to be evaluated at the boundary conditions.

5.3 Dimensionless Inner Boundary Condition in Terms of Dimensionless Pressure and Transmissibility

Equation 5.19 still has an unknown variable α which needs to be determined. The the inner boundary condition, expressed in terms of Darcy's law for mass flowrate is given as

$$\rho_i \rho_n(p) q_{sf}(p) = \frac{2\pi k_i h_i \rho_i}{\mu_i} T_n(p) r_D \frac{\partial p}{\partial r_D} \tag{5.21}$$

Including dimensionless pressure, from equation 5.19

$$\rho_n(p) B(p) q_{sc}(p) = -\frac{2\pi k_i h_i}{\mu_i} T_n(p) \alpha r_D \frac{\partial p_D}{\partial r_D} \tag{5.22}$$

This equation includes the unknown α. Note that the volume rate is now at standard conditions and therefor the formation volume factor is included. By moving all terms to the right hand side

$$1 = -\frac{2\pi k_i h_i}{q_{sc}(p) \mu_i \rho_n(p) B(p)} T_n(p) \alpha r_D \frac{\partial p_D}{\partial r_D} \tag{5.23}$$

By also noting that the normalized permeability times formation volume factor is equal to the initial formation volume factor (see Appendix B for details) B_i this simplifies to

$$1 = -\frac{2\pi k_i h_i}{q_{sc}(p)\mu_i B_i} T_n(p) \alpha r_D \frac{\partial p_D}{\partial r_D} \tag{5.24}$$

From the conventional inner boundary condition

$$\left[r_D \frac{\partial p_D}{\partial r_D} \right]_{r_D=1} = -1 \tag{5.25}$$

the inner boundary condition for this problem must be

$$\left[r_D \frac{\partial p_D}{\partial r_D} \right]_{r_D=1} = -T_n(p) \tag{5.26}$$

and hence the value of α is

$$\alpha = \frac{q_{sc}\mu_i B_i}{2\pi k_i \mu_i} \tag{5.27}$$

That concludes the inner boundary condition calculations for p_D but the inner boundary condition for T_n is also desired. Again starting with the extended form of Darcy's law

$$q_{sc}(p) = -\frac{2\pi k_i h_i}{\mu_i B_i} T_n(p) r_D \frac{\partial \Delta p}{\partial r_D} \tag{5.28}$$

Referring back to equation 5.9 to find the relationship

$$d\Delta p = \frac{1}{\tau T_n} d\Delta T_n \tag{5.29}$$

Substitution of this equation into Darcy's law results in

$$q_{sc}(p) = -\frac{2\pi k_i h_i}{\mu_i B_i \tau} r_D \frac{\partial \Delta T_n}{\partial r_D} \tag{5.30}$$

and

$$r_D \frac{\partial \Delta T_n}{\partial r_D} = -\frac{q_{sc}(p)\mu_i B_i \tau}{2\pi k_i h_i} \tag{5.31}$$

Which can be expressed as

$$r_D \frac{\partial \Delta T_n}{\partial r_D} = -\tau_D \tag{5.32}$$

The relationship between τ_D and p_D is found by equation 5.29

$$\frac{2\pi k_i h_i}{q_{sc}\mu_i B_i} d\Delta p = \frac{2\pi k_i h_i}{q_{sc}\mu_i B_i} \frac{1}{\tau T_n} d\Delta T_n \tag{5.33}$$

which in turn simplifies and gives the relationship

$$p_D = \frac{1}{\tau_D T_n} d\Delta T_n \tag{5.34}$$

5.4 Deriving the Solution Using the Exponential Integral Function

From 5.20 the diffusivity equation is found in terms of dimensionless pressure. To derive a E_i solution the diffusivity equation needs to be expressed in terms of the transmissivity. By rearranging equation 5.20, knowing now the relationship between dimensionless pressure and transmissivity from 5.34

$$\frac{1}{r_D} \frac{\partial}{\partial r_D} \left(T_n(p) r_D \frac{1}{\tau_D T_n(p)} \frac{\partial \Delta T_n}{\partial r_D} \right) = \frac{1}{\tau_D T_n(p)} \frac{\partial \Delta T_n}{\partial t_D} \tag{5.35}$$

which again simplifies to

$$\frac{\partial}{\partial r_D} \left(r_D \frac{\partial \Delta T_n}{\partial r_D} \right) = \frac{1}{T_n(p)} \frac{\partial \Delta T_n}{\partial t_D} \tag{5.36}$$

Evaluation at initial conditions gives $T_n(p_i) = 1$ and results in

$$\frac{\partial}{\partial r_D} \left(r_D \frac{\partial \Delta T_n}{\partial r_D} \right) = \frac{\partial \Delta T_n}{\partial t_D} \tag{5.37}$$

With the inner boundary condition

$$r_D \frac{d\Delta T_n}{dr_D} = -\tau_D \text{ when } r_D = 1 \tag{5.38}$$

or for the line source solution

$$r_D \frac{d\Delta T_n}{dr_D} = -\tau_D \text{ when } r_D \rightarrow 0 \tag{5.39}$$

The initial condition

$$\Delta T_n \rightarrow 0 \text{ when } t_D \rightarrow 0 \tag{5.40}$$

and the outer boundary condition

$$\Delta T_n \rightarrow 0 \text{ when } r_D \rightarrow \infty \tag{5.41}$$

The solution of 5.37 using the conditions above gives the E_i solution

$$\Delta T_n = -\frac{\tau_D}{2} E_i \left(-\frac{{r_D}^2}{4t_D} \right) \tag{5.42}$$

which may be converted back to pressure by (see Appendix A for details), and gives the final result

$$p_D = -\frac{1}{\tau_D} \ln \left[1 + \frac{\tau_D}{2} E_i \left(-\frac{{r_D}^2}{4t_D} \right) \right] \tag{5.43}$$

$$p_D = -\frac{1}{\tau_D} \ln \left(1 + \Delta T_n \right) \tag{5.44}$$

Equation 5.43 is the drawdown dimensionless pressure solution. A plot of p_D versus $\frac{t_D}{{r_D}^2}$, known as a plot for interference test, may be found by this solution

To obtain the build up solution the principle of superposition is applied to the expression of ΔT_n so that the buildup expression is

$$\Delta T_{n,BU} = -\frac{\tau_D}{2}\left\{E_i\left(-\frac{{r_D}^2}{4(t_D+\Delta t_D)}\right) - E_i\left(-\frac{{r_D}^2}{4\Delta t_D}\right)\right\} \tag{5.45}$$

$$p_{D,BU} = -\frac{1}{\tau_D}\ln\left(1+\Delta T_{n,BU}\right) \tag{5.46}$$

$$p_{D,BU} = -\frac{1}{\tau_D}\ln\left[1+\frac{\tau_D}{2}\left\{E_i\left(-\frac{{r_D}^2}{4(t_D+\Delta t_D)}\right) - E_i\left(-\frac{{r_D}^2}{4\Delta t_D}\right)\right\}\right] \tag{5.47}$$

The solution for drawdown wellbore pressure can then be found by knowing that

$$(p_i - p) = -\frac{1}{\tau}\ln(1-\Delta T_n) \tag{5.48}$$

resulting in

$$p_w = p_i + \frac{1}{\tau}\ln(1-\Delta T_n) \tag{5.49}$$

and for build up wellbore pressure

$$p_w = p_i + \frac{1}{\tau}\ln(1-\Delta T_{n,BU}) \tag{5.50}$$

5.5 Deriving the Laplace Solution for Storage and Skin

A solution including storage and skin was represented by Kikani and Pedrosa (1991). For this case the solution including storage and skin is slightly different. It is a time consuming operation to obtain the new solution from the governing equation. By noting that the difference between the current solution and the solution of Kikani and Pedrosa (1991) lies in the inner boundary condition.

From Kikani and Pedrosa (1991) : $r_D\frac{\partial n}{\partial r_D} = -1$

From current solution: $r_D\frac{\partial \Delta T_n}{\partial r_D} = -\tau_D$

The relationship between the two solutions can be expressed as

$$\Delta T_n = \tau_D n \tag{5.51}$$

given that

$$n = \frac{1}{\tau_D} \Delta T_n \tag{5.52}$$

The resulting Laplace space equation for the current solution is then given as

$$\Delta T_n \tau_D = \frac{K_0\left(\sqrt{s}\right) + S\left(\sqrt{s}\right) K_1\left(\sqrt{s}\right)}{s\left\{\sqrt{s} K_1\left(\sqrt{s}\right) + sC_D\left[K_0\left(\sqrt{s}\right) + \sqrt{s} K_1\left(\sqrt{s}\right)\right]\right\}} \tag{5.53}$$

Which can be inverted back to time domain by use of Stefhest Algorithm, section 4.1.3.3.

The solution without storage and skin can easily be expressed in Laplace space by

$$\Delta T_n \tau_D = \frac{K_0\left(\sqrt{s}\right)}{s\left\{\sqrt{s} K_1\left(\sqrt{s}\right)\right\}} \tag{5.54}$$

Chapter 6

Results and Evaluation

6.1 Verification of New Model

To verify the results represented above the zero-order E_i solution of Kikani and Pedrosa (1991) is used as a base, and implemented in MATLAB for different values of τ_D. These curves are compared against the buildup solution using the E_i function, equation 5.47, and the Laplace solution, equation5.54, (Chapter 5). In these solutions $\tau_D = 0.25$.

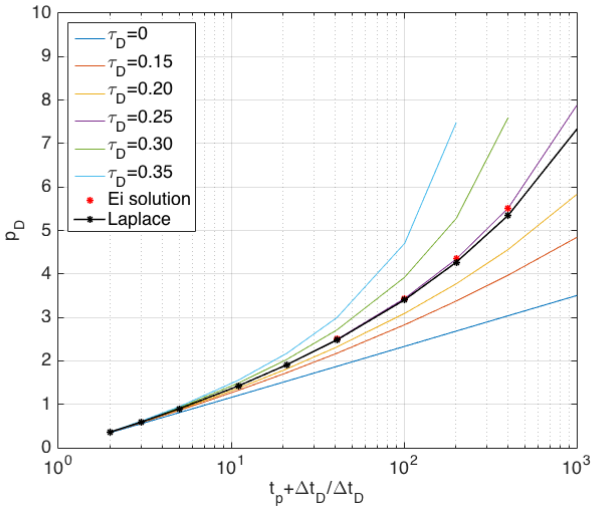

Figure 6.1: Horner type curve with comparison of Kikani and Pedrosa (1991) solution against new developed E_i and Laplace solution for $\tau_D = 0.25$

As can be seen from figure 6.1, the E_i build up solution match very well to the solution of Kikani and Pedrosa (1991) and the Laplace solution also matches quite well. The Laplace space solution is known to give the most accurate approximation, Jelmert (2015), so this may actually indicate that the two other solutions are not as accurate. Moreover the Laplace solution enables the inclusion of storage and skin effects, represented later in chapter 6.

On the other hand the E_i solution found in equation 5.47 is easier to handle and also readily implemented in MATLAB using the built-in ei solver. Therefor this solution will be used for investigation of thickness changes near the wellbore and to represent the interference test curves for the stress-sensitive case.

6.2 Field Case

For the study of compressibility change effecting the height and consequently the stress sensitivity parameter of the height change, the article of Chen and Li (2008) is used as reference for field data. They present a field case of the Qingxi oilfield, known to be prone for stress sensitivity.

6.2.1 Deformation Coefficient

R.Raghavan et al. (1972) express the height in terms of bulk volume and compressibility. They define the bulk volume as $\delta_x \delta_y h$, the relative volume in x and y direction times thickness. From the equation of porosity to volume

$$\phi = \frac{V_p}{V_b} \tag{6.1}$$

where the pore volume can be expressed as $V_P = \delta_x \delta_y h \phi$

R.Raghavan et al. (1972) assumes that compaction or expansion only occurs in the vertical direction and express the pore volume compressibility as,

$$c_f = \frac{1}{V_p} \left(\frac{\partial V_p}{\partial p} \right)_T \tag{6.2}$$

which again can be expressed as

$$c_f = \frac{1}{h(p)\phi(p)} \left(\frac{\partial(h\phi)}{\partial p} \right)_T \tag{6.3}$$

From the reported Young's modulus and Poisson's ratio of the Qingix field, Chen and Li (2008), one can find the bulk modulus. The formula for bulk modulus, K, is given by

$$K = \frac{E}{3(1-2\nu)} \tag{6.4}$$

where E represents the Young's modulus and ν Poisson's ratio. The bulk modulus K is equivalent to the inverse of the compressibility, which again is dependent on height and porosity, as shown in equation6.3. The equation of the height change due to pressure is given by

$$h = h_i e^{\xi(p_w - p_i)} \tag{6.5}$$

where ξ is the height modulus, also represented in chapter 5 by equation 5.2d. By the definition the compressibility in equation 6.3 it is assumed that the value of ξ is that of the inverse bulk modulus compressibility, so that

$$K \approx \frac{1}{\xi} \tag{6.6}$$

From the semester project, Lillehammer (2014) τ was expressed as a product of the different pressure dependent variables modulus

$$\tau = \gamma + c + \xi - \nu \tag{6.7}$$

The value of τ can be estimated when the value of ξ is known from the bulk modulus, and assuming that γ and ν can be found by lab measurements and c by correlations or PVT analysis. The latter is also assumed in the article of Kikani and Pedrosa (1991) and shown in the semester project, Lillehammer (2014).

For the field case presented here, the only value available is the height modulus found from

the inverse bulk modulus as shown equation 6.6. Assuming that ξ contributes to a certain part of the total τ value, an approximate value of τ is achieved and can be used in further calculations. Reservoir parameters for the Qingxi field can be found in table 6.1

Table 6.1: Reservoir parameters for Qingxi oilfield used to calculate ξ and thereby find τ_D

Parameter	**Unit**	**Value**
Permeability	μm^2	$100 \cdot 10^{-3}$
Formation thickness	m	13.51
Reservoir pressure	MPa	56.0
Bubblepoint pressure	MPa	22.0
Oil viscosity under reservoir conditions	mPa·s	5.73
Rw	m	0.15
Re	m	150
Young's modulus	MPa	689.48
Poisson's ratio	-	0.20
Formation volume factor	-	1.20

Table 6.2 shows values used to solve for τ_D when ξ is assumed to correspond to half of the total τ value. This results in $\tau_D = 0.0073$ for an assumed flow rate of $150 m^3/d$. The value of τ_D using the data from the Qingxi field does in other words depend on two assumptions, the value difference between ξ and τ and the flow rate.

Table 6.2: Illustration of approach to find value of τ_D

Eq. with symbols	**Eq. with values**	**Final value**	**Unit**
$K = \frac{E}{3(1-2\nu)}$	$K = \frac{689.48}{3(1-2*0.2)}$	$K = 383$	[Mpa]
$\xi = \frac{1}{K}$	$\xi = \frac{1}{383*10^6}$	$\xi = 2.6 * 10^-9$	$[\frac{1}{pa}]$
$\tau_D = \frac{q_{sc}\mu_i B_i 2 \cdot \varsigma}{2\pi k_i h_i}$	$\tau_D = \frac{0.0017[m^3/s] \cdot 0.0057[pas] \cdot 1.2 \cdot 2 \cdot 2.61 \cdot 10^{-9}}{2\pi, \cdot 1 \cdot 10^{-13}[m^2] \cdot 13.51[m][pa]}$	$\tau_D = 0.0073$	[-]

As τ depends on several parameters it is reasonable to assume that τ is larger than ξ. The size of τ to ξ is from here on described as a "size factor", S, where S in the current example is 2, see table 6.2.

The flow rate is determined based on the maximum flow rate for one of the wells in the article of Chen and Li (2008)(figure 6), see also table 6.2. Typical well flowing rates can vary greatly. Onshore fields have oil flow rates ranging from 50 to $450 m^3/day$ while offshore fields have oil flow rates ranging from 300 to $1000 m^3/day$, according to Snoeks (2015). Gas rates are usually higher.

6.2.2 Resulting Deformation

With the given reservoir parameters an investigation of how the height is affected by the height modulus ξ and the pressure change, $p_w - p_i$ is done, represented by equation 6.5. The pressure at the well can be found by equation 5.49 for the drawdown solution and 5.50 for the buildup solution, also included below for convenience.

For drawdown

$$p_w = p_i + \frac{1}{\tau} \ln(1 - \Delta T_n) \tag{6.8}$$

and for build up

$$p_w = p_i + \frac{1}{\tau} \ln(1 - \Delta T_{n,BU}) \tag{6.9}$$

Note that for the drawdown and buildup solution the dimensionless radius, r_D is assumed to be 1 as investigation is done for the pressure at the well.

The height change expressed by equation 6.5 is found both for the drawdown and buildup solution. This equation can be solved knowing the height modulus,ξ and initial pressure,p_i and assuming a value of τ and thereby τ_D. An illustration of the compaction of a stress sensitive reservoir as shown in figure 6.2. Figure 6.2a represents the drawdown solution and figure 6.2b the buildup solution. For the drawdown solution it is observed that the predicted height decreases linearly as the reservoir is depleted and well pressure, p_w decreases. For the buildup solution on the other hand the height and well bore pressure increases linearly.This is indicated by the arrows in figure 6.2.

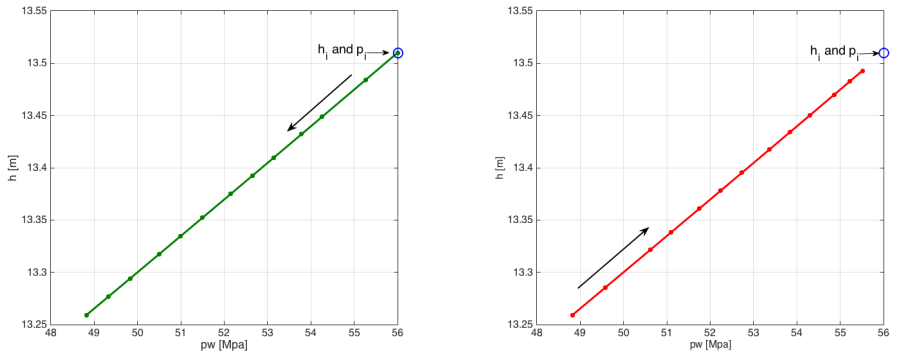

(a) Drawdown solution causing reservoir height decrease

(b) Buildup solution causing reservoir height increase

Figure 6.2: Drawdown and buildup solutions showing decrease and increase in reservoir height when $\tau_D = 0.0073$ and q = 150 m^3/d

In this model, elastic deformation is assumed. This means that the deformation is assumed possible in both negative and positive direction. From figure 6.2b it can be observed that the last point in the buildup solution does not reach all the way to the initial value, but stops below. Figure 6.3 includes both the drawdown and buildup solution, illustrating even clearer that the two solutions do not share the exact same values. From table 6.3 it can be seen that the first values of the drawdown solution is equal to the initial values of the Qingxi oilfield, while the last buildup values are smaller than initial pressure and height values, indicated by red in table 6.3.

To get an even better understanding of the difference in the drawdown and buildup solution from the height versus pressure plots, the change in thickness is plotted against dimensionless time. As can be seen from figure 6.4 the deformation with time is negative for drawdown and positive for build up pressure. This proves that a decrease in pressure will cause compaction whilst an increase in pressure will cause a rise in the formation. From 6.4 the initial height is marked by a blue and dotted line, illustrating again that the buildup solution does not reach initial values at any time. The formation does not revert fully back to the nitial height of 13.51 meters. This indicates that even though the formation is assumed elastic, it can not be completely reversed in the positive thickness direction.

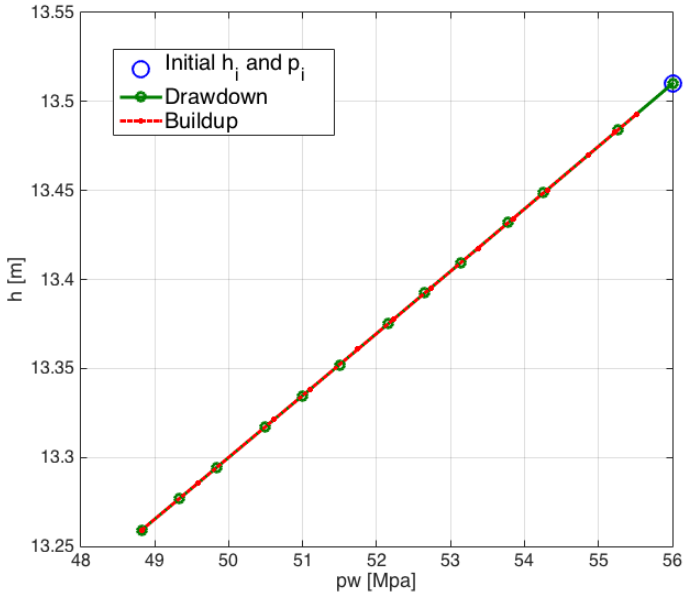

Figure 6.3: Drawdown and buildup solutions showing decrease and increase in reservoir height when $\tau_D = 0.0073$ and q = 150 m^3/d

Table 6.3: Drawdown and buildup values for Qingxi oilfield when $\tau_D = 0.0073$ and q = 150 m^3/s

Drawdown		**Buildup**	
pw [Mpa]	h [m]	pw [Mpa]	h [m]
56.0	13.51	48.8	13.26
55.3	13.48	49.6	13.29
54.3	13.45	50.6	13.32
53.8	13.43	51.1	13.34
53.1	13.41	51.7	13.36
52.6	13.39	52.2	13.38
52.2	13.37	52.7	13.40
51.5	13.35	53.4	13.42
51.0	13.33	53.8	13.43
50.5	13.32	54.3	13.45
49.8	13.29	54.9	13.47
49.3	13.28	55.2	13.48
48.8	13.26	55.5	13.49

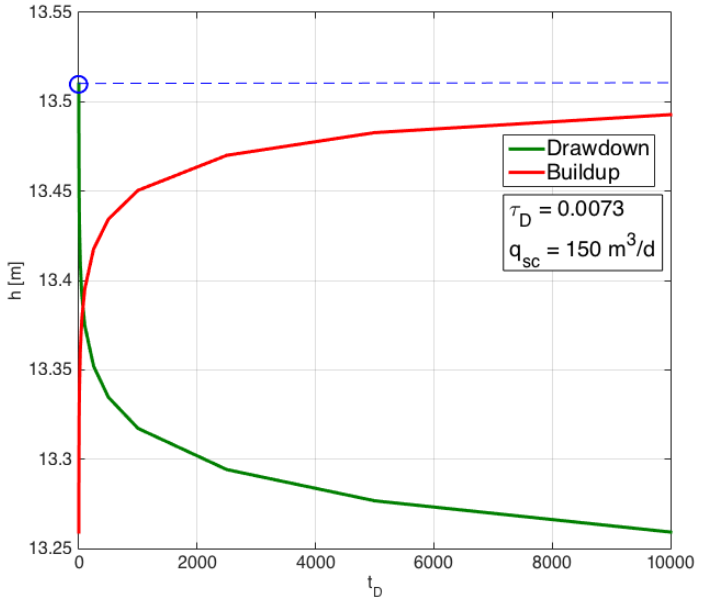

Figure 6.4: Thickness change with dimensionless time for drawdown and buildup solution when $\tau_D = 0.0073$ and q = 150 m^3/d. The height decreases more during drawdown than it increases during buildup

Figures 6.2 - 6.4, all assume a stress-sensitive modulus, τ_D, of 0.0073. From previous studies, Kikani and Pedrosa (1991), the stress-sensitivity can be higher than this. The same solutions are therefor plotted for a τ_D value of 0.1273, found by setting the size factor S = 8 and the flow rate to 650 m^3/d. The resulting deformation for drawdown and buildup can be observed from figure 6.5 comparing the solution for a τ_D value of 0.0073 against a τ_D value of 0.1284. Figure 6.5a and 6.5b shows the drawdown solution and the buildup solution respectively.

It is observed that the deformation increases as stress-sensitivity is increased, as is also expected. The deformation for both the drawdown and buildup solution against dimensionless time is illustrated in figure 6.6, for $\tau_D = 0.1273$. The plot indicates that increase stress sensitivity causes increased compaction for the drawdown solution. For the case of buildup on the other hand the rise is less for a larger stress-sensitivity parameter. This can be seen even clearer when plotting the two stress-sensitive cases against each other, illustrated in figure 6.7

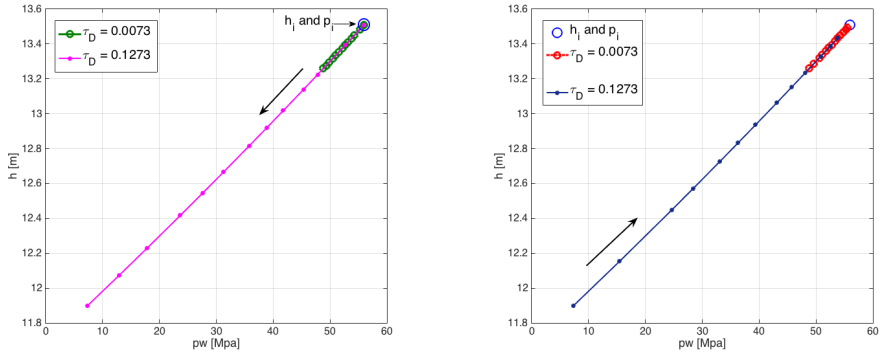

(a) Drawdown solutions for $\tau_D = 0.0073$ and $\tau_D = 0.1273$

(b) Buildup solutions for $\tau_D = 0.0073$ and $\tau_D = 0.1273$

Figure 6.5: Drawdown and buildup solutions comparing amount of height decrease and increase, respectively, for two degrees of stress-sensitivity

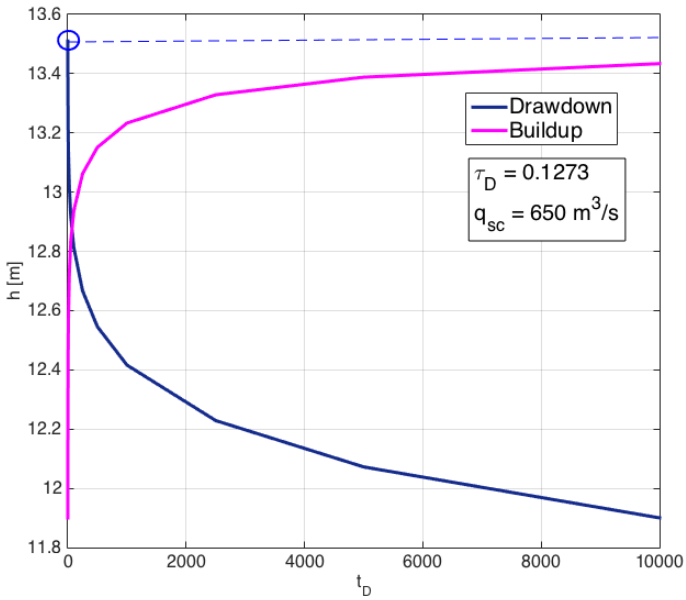

Figure 6.6: Thickness change with dimensionless time for drawdown and buildup solution when$\tau_D = 0.1273$ and q = 650 m^3/d

Table 6.4: Drawdown and buildup values for Qingxi oilfield when $\tau_D = 0.1273$ and q = 650 m^3/s

Drawdown		Buildup	
pw [Mpa]	h [m]	pw [Mpa]	h [m]
56.0	13.51	7.4	11.90
52.7	13.39	15.5	12.15
47.8	13.22	24.6	12.45
45.3	13.14	28.4	12.57
41.8	13.02	33.0	12.72
38.9	12.92	36.3	12.83
35.8	12.81	39.4	12.94
31.3	12.67	43.1	13.06
27.6	12.55	45.7	13.15
23.7	12.42	48.1	13.23
17.8	12.23	50.8	13.33
12.9	12.07	52.5	13.39
7.4	11.90	53.8	13.43

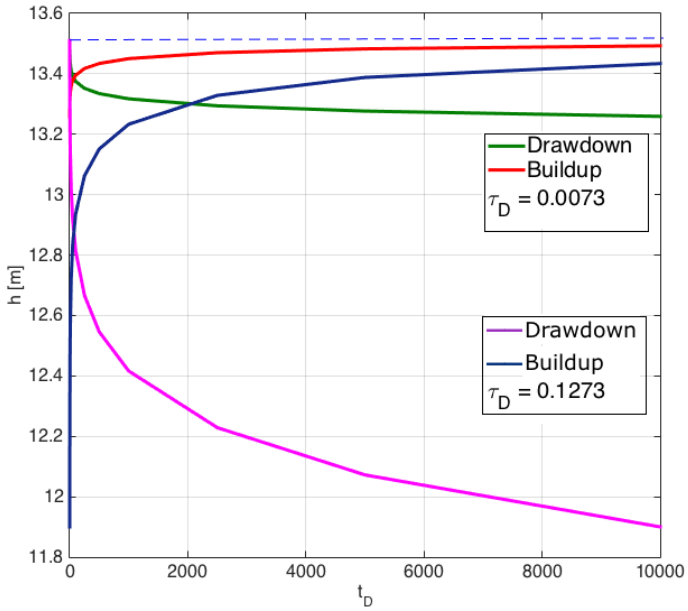

Figure 6.7: Comparison of thickness change with dimensionless time for drawdown and buildup solutions with two degrees of stress-sensitivity

6.3 Sensitivity Analysis

6.3.1 Value of Stress-Dependent Parameter τ_D

As mentioned earlier the value of τ_D using the data from the Qingxi field depend on the assumption of size factor for ξ to τ and flow rate. The other variables to determine τ_D is tabulated in table 6.1.

Figure 6.8 illustrates a range of τ_D values when dependent on ξ by a changing size factor and different constant flow rates. The two τ_D values used in section 6.2.2 are marked by red circles in the figure. It is observed that the value of constant flow rate assumed has a large effect on the stress-sensitive parameter τ_D, as well as the size factor.

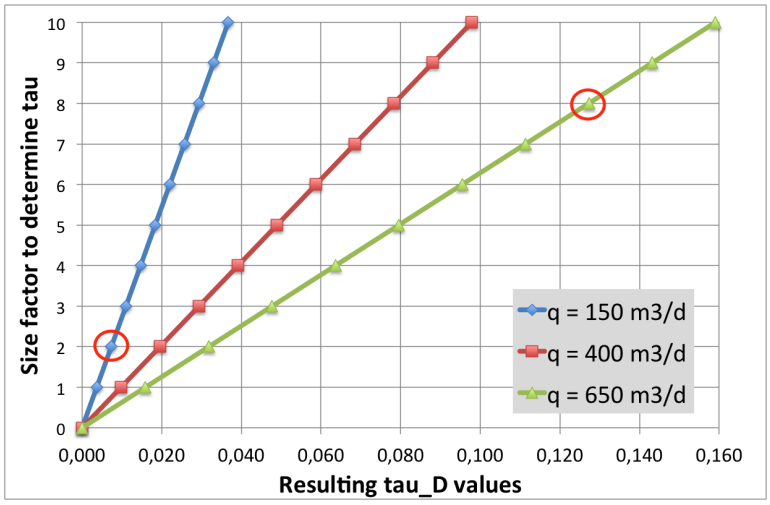

Figure 6.8: Range of values of τ_D versus the size factor of ξ to τ for different flow rates

6.3.2 Interference Test

A plot for the interference test is produced from the drawdown solution

$$p_D = -\frac{1}{\tau_D} \ln \left[1 + \frac{\tau_D}{2} E_i \left(-\frac{{r_D}^2}{4t_D} \right) \right] \tag{6.10}$$

plotted against the dimensionless time over dimensionless radius squared, $\frac{t_D}{{r_D}^2}$. The interference test is commonly used to determine pressure communication between wells and subsequently the permeability and porosity-compressibility product if communication exists. It is therefor of interest to express the interference test curve of a stress-sensitive reservoir against that of a homogeneous reservoir. The homogeneous solution is plotted together with the stress-sensitive solution, where the latter is plotted for several values of τ_D, as seen in figure 6.9.

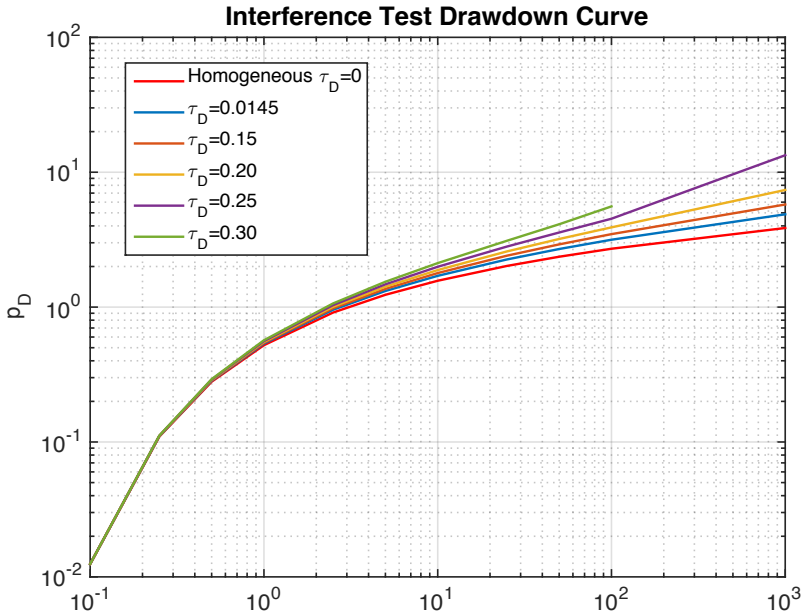

Figure 6.9: Interference test results at different values of τ_D. Comparing the homogeneous solution against several degrees of stress-sensitivity

From figure 6.9 it is observed that all the solutions are equal for early time behavior and then the stress-sensitive solution deviates more the larger the τ_D value becomes. The deviation at late time is more or less constant for values of τ_D between 0 to 0.20. The

interval is approximately 1 on the log log scale between the curves. However, at a τ_D value of 0.25, the late time result has a greater vertical interval.

From figure 6.9 it can be noted that the curve for $\tau_D = 0.30$ does not exist for $\frac{t_D}{{r_D}^2}$ values higher than 10^2. This is because the results give imaginary numbers for high τ_D at large values of time. These values are therefor disregarded by MATLAB code as they do not give any sensible values for interpretation.

A clear trend is shown from the interference test, the larger the τ_D value the more deviation from the homogeneous solution. For this plot the value of the dimensionless radius, r_D is assumed to be 10.

In figure 6.9 the dimensionless radius is assumed constant. For this study it is also of interest to plot the dimensionless radius for different values and compare the stress-sensitive and homogeneous solution. This type of plot can be used to find the equivalent wellbore radius, r_{we}, used to represent the skin factor mathematically instead of as a pressure drop.

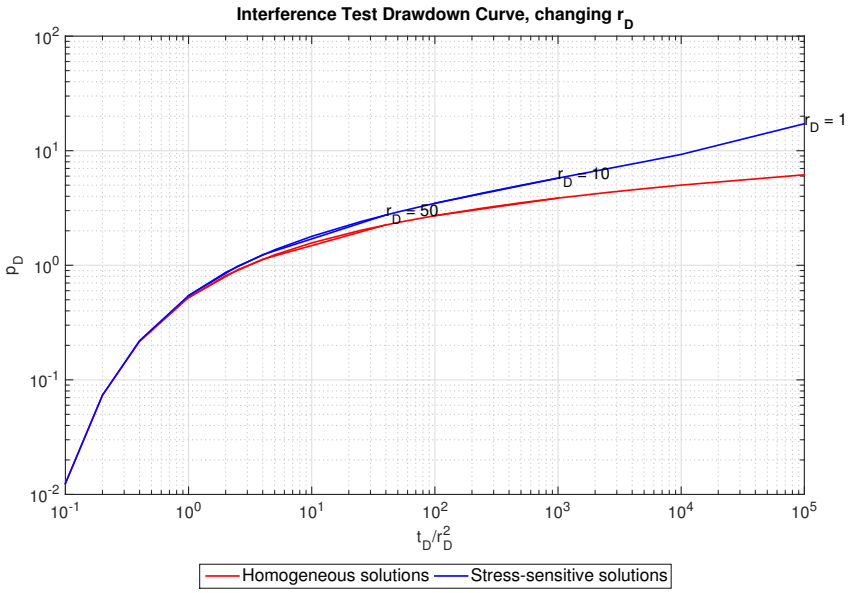

Figure 6.10: Interference test results at different values of r_D

Figure 6.10 illustrates the interference solution for three cases of dimensionless wellbore radius. At early times the homogeneous and stress-sensitive solutions increase at the same

rate. As time increases the stress-sensitive solution deviates more and more. Indicating that the resulting equivalent wellbore radius will differ in the case of stress-sensitivity compared to assuming homogeneous conditions. The three r_D values marked on the figure are each at the maximum value of x- and y-coordinates. This is true both for the stress-sensitive and the homogeneous case. This again shows that for a dimensionless radius of $r_D = 50$ the solution is only valid for short times, while it is valid for longer time intervals for $r_D = 1$. For values of r_D larger than 50 the solution becomes inconsistent, and does not show any clear trend. The plot in figure 6.10 is therefor best fitted for wells spaced close together where a short radial distance is expected.

6.3.3 Including Wellbore Storage and Skin

The solution including wellbore storage and skin is represented in chapter 5 by equation 5.53. This solution is compared against the line source solution with storage and skin, represented in chapter 4 by equation 4.38. When τ_D is very small the two solutions are equal.

The effect of storage is seen on the early time data, as illustrated in figures 6.11 and 6.12. The effect of skin is seen on the late time data, as illustrated in figures 6.13 and 6.14.

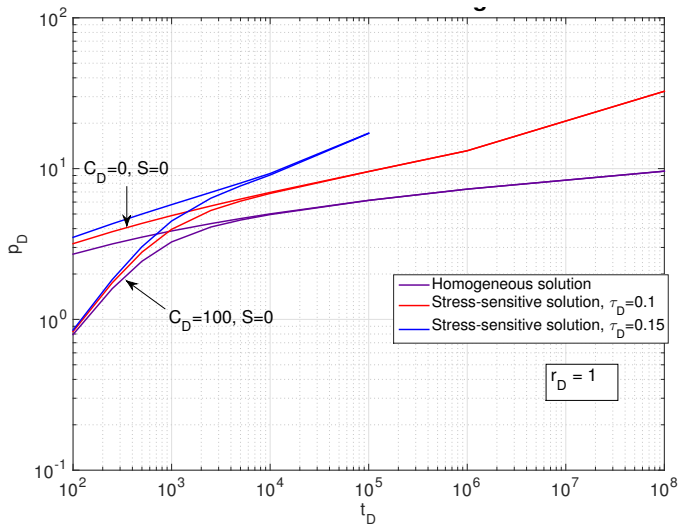

Figure 6.11: Comparison of homogeneous and stress-sensitive solution for $C_D = 0$ versus $C_D = 100$ for two values of τ_D

From figure 6.11 it is observed that including stress-sensitivity causes a higher increase in pressure. This pressure increase is enhanced by the increase of τ_D. For the case of no storage, the pressure increase is seen also for the early time data. By including storage the homogeneous and stress sensitive solutions are similar at early times but deviates at intermediate and late times. The pressure increase from intermediate times and late times is the same for no storage and storage solutions.

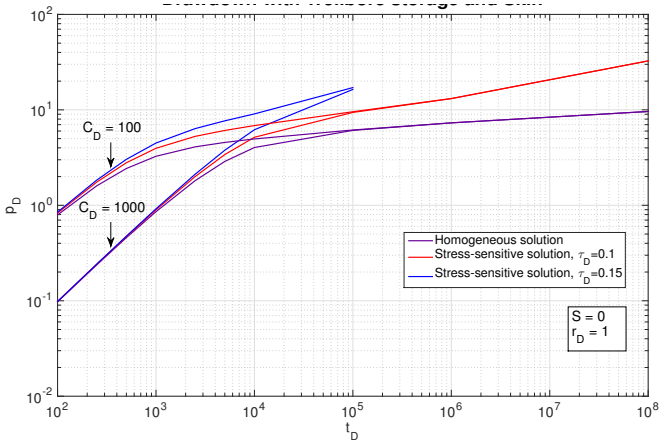

Figure 6.12: Comparison of homogeneous and stress-sensitive solution for $C_D = 100$ versus $C_D = 1000$ for two values of τ_D

Figure 6.12 shows much of the same effects as 6.11. For a wellbore storage constant, $C_D = 1000$, it is observed that the early time unit slope line is not affected by stress-sensitivity. For $\tau_D = 0.15$ the solution is only valid for early and intermediate times. After this the solution becomes imaginary, as it does not give any reliable data. The latter part is neglected in MATLAB.

Figure 6.13 illustrates solutions including skin and storage. At a value of skin of only five, the plot is similar to that of figure 6.12. It should be noted that the degree of stress-sensitivity has to be lowered to get sensible values in the model.

Including only skin will produce almost horizontal lines that will be shifted downwards or upwards depending on whether the solution is homogeneous or stress-sensitive, and depending on degree of stress-sensitivity.

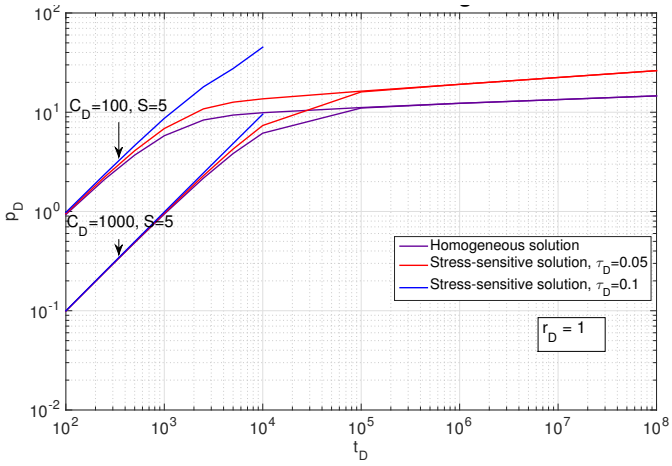

Figure 6.13: Comparison of homogeneous and stress-sensitive solution for $C_D = 100$ and S= 5 versus $C_D = 1000$ and S = 5 for two values of τ_D

By increasing the value of skin to 20, as illustrated in figure 6.14 the effect of skin is clearly visible. This produces two curves that do not meet at any point in time, unlike the other examples above. The stress-sensitivity parameter, τ_D has to be decreased even more to produce sensible values. For the stress-sensitive solution, $\tau_D = 0.03$ the dimensionless pressure reaches a value close to 100 at late times.

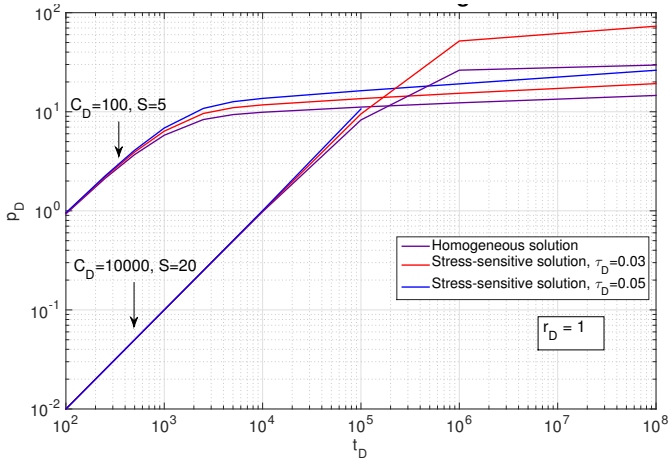

Figure 6.14: Comparison of homogeneous and stress-sensitive solution for $C_D = 100$ and S= 5 versus $C_D = 10000$ and S = 20 for two values of τ_D

Chapter 7

Further Discussion and Evaluation

In the new stress-sensitive model all pressure dependent moduli are assumed constant and the combined variable T_n are assumed to vary exponentially. This is an approximation, and thus will not give an exact result, which is important to keep in mind.

In the literature review several other ways to estimate the permeability as a function of pressure where mentioned. Describing the permeability, and possibly other variables, by the stepwise of two-parameter exponential function, might give more precise results, but would also further complicate the calculation to linearize the diffusivity equation.

The deformation model represented in chapter 6 is used to predict the possible compaction thus also depend upon several assumptions. The resulting plotted data therefor only shows predictions of theoretical behavior.

The drawdown and buildup deformation for a τ_D value of 0.1273 also results a large wellbore pressure change over the reservoir height change range. If τ_D is further increased, the model will predict negative wellbore pressures at lower heights, and thus it is no longer reliable.

Compaction in reservoirs can benefit the recovery of hydrocarbons by providing extra energy, but more often than not compaction causes field-operating problems. Casing collapse is a known problem in fields with large amounts of compaction. As the formation moves it may pull the cemented casing with it, causing compression in this part of the casing. Above the formation compacting the casing will be elongated creating stretch in the cas-

ing Doornhof et al. (2006)

When doing sensitivity analysis on the new developed solutions it is found that for large values of the stress-sensitivity parameter, τ_D, the results are not always reliable. At intermediate and late times the values become partly imaginary numbers, which cannot be used to get any valuable data. This is a limiting feature of the model.

7.1 further work

- The new solution can be investigate to an even wider extent, looking at the behavior of the solution for a constant pressure test. The dimensionless flowrate has to be found by Laplace transformation or convolution.
- For the model including storage and skin the solution could also be expressed by a Gringarten type curve. This is a plot of p_D versus $\frac{t_D}{C_D}$ and is extensively used in the petroleum industry.
- The model for deformation could be tested for a stress-sensitive reservoir where compaction close to the well has occurred. This could be used to further confirm if the theoretical behavior found here resembles real field results and thus giving confidence for further development.
- If solutions for the pressure derivatives can be found the solutions can also be expressed by diagnostic plots. A major application of diagnostic plots is to determine different flow regimes in a buildup or flow test.
- A similar equation for fracture flow in Cartesian coordinates can also be developed, and with some modification put into the same MATLAB scrip's, as much of the implementation will be similar.

Chapter 8

Conclusion

- A new form of the diffusivity equation including the pressure dependency of permeability, viscosity, fluid density and thickness is derived. The model gives sensible results both for drawdown and buildup solution, according to previous similar work.
- The new form of the diffusivity equation is solved by the use of the exponential integral, and also by Laplace transformation when including storage and skin.
- The solution is best fit for new wells, giving an early prediction of the expected productivity before additional reservoir information is available.
- The deformation thickness for drawdown and buildup is found as a straight line. The difference between the two solutions shows that deformation cannot be completely reversed in the case of build up pressure.
- The deformation model also shown that by increasing stress-sensitivity the deformation during drawdown is increased while the reverse deformation during buildup is further decreased.
- Interference test for the drawdown solution shows that an increase in τ_D cases an increased deviation from the homogeneous solution.
- An interference test for varying r_D results in a continuous line, as long as the dimensionless radius is not larger then approximately 50. This plot can be used to find the equivalent wellbore radius.
- The model can also be used for wells with storage and skin, by updating the Laplace space solution of Kikani and Pedrosa (1991) to fit the new boundary conditions. The

solution in time domain can be found by the use of Stefhest algorithm.

- The graphical representations including storage and skin shows that the stress-sensitivity does not effect the early time unit slope for wellbore storage. This has also been found from other studies and gives greater confidence that the storage coefficient C can still be found by the unit slope in a stress sensitive formation.
- At intermediate and late times stress sensitivity effects both the solution for only storage and also the solution with storage and skin combined.
- The pressure predictions given by the current model are believed to give more reliable values than the use of a homogeneous solution when encountered with a stress sensitive reservoir.

Nomenclature

Symbol	Units	Description
B	$-$	Formation volume factor
c	1/Pa	Compressibility
c_f	1/Pa	Formation compressibility
c_i	1/Pa	Initial compressibility
c_t	1/Pa	Total compressibility
E	Pa	Young's modulus
C_D	$-$	Dimensionless wellbore storage constant
$E_i(z)$	$-$	Exponential integral function
h	m	Formation thickness
h_i	m	Initial formation thickness
I_0	$-$	Modified Bessel function of first kind, zero order
k	m^2	Permeability
k_i	m^2	Initial permeability
K	Pa	Bulk modulus
K_0	$-$	Modified Bessel function of second kind, zero order
K_1	$-$	Modified Bessel function of second kind, first order
p	Pa	Pressure
p_D	$-$	Dimensionless pressure
p_e	Pa	Pressure at outer boundary
p_i	Pa	Initial pressure
p_{wf}	Pa	Well flowing pressure
p_{ws}	Pa	Well shut-in pressure
q	m^3/s	Flowrate
q_{sc}	m^3/s	Sandface Flowrate
r	m	Radial distance
r_D	$-$	Dimensionless radial distance
r_e	m	Reservoir outer boundary radial distance
r_w	m	Wellbore radius

r_{we}	m	Equivalent wellbore radius
S	–	Skin
t	s	Time
t_D	–	Dimensionless time
t_{pD}	–	Dimensionless producing time
T_i	–	Initial Transmissivity
T_n	–	Normalized Transmissivity
$T(p)$	–	Transmissivity

Greek Symbols

Symbol	**Units**	**Description**
α	1/Pa	Porosity modulus
γ	1/Pa	Permeability modulus
γ_D	1/Pa	Dimensionless
Δt	s	Shut-in time
Δt_D	–	Dimensionless shut-in time
ΔT_i	–	Initial Transmissivity
ΔT_n	–	Normalized Transmissivity
$\Delta T(p)$	–	Transmissivity
η	1/Pa	Pressure dependent variable
μ	Pa s	Viscosity
ν	–	Poisson ratio
ξ	1/Pa	Thickness modulus
ρ	kg/m^3	Density
τ	1/Pa	Combined pressure dependent modulus
τ_D	1/Pa	Dimensionless combined pressure dependent modulus
υ	1/Pa	Viscosity Modulus
ϕ	–	Porosity

References

Agarwal, R. G., Al-Hussainy, R., Jr, H. R., 1970. *An Investigation of Wellbore Storage and Skin Effect In Unsteady Liquid Flow, Analytical Treatment*. Tech. rep., Society of Petroleum Engineers.

Ahmed, T., 2001. *Reservoir Engineering Handbook*. Elsevier.

Ambastha, A., Zhang, M. Y., 1996. *Iterative and numerical solutions for pressure-transient analysis of stress-sensitive reservoirs and aquifers*. Vol. Volume 22, Issue 6. Elsevier, doi:10.1016/0098-3004(95)00114-X.

Bourdet, D., 2002. *Well Test Analysis - The Use of Advanved Interpretation Models*. Elsevier.

Chen, S., Li, H., 2008. *A New Technique for Production Prediction in Stress-Sensitive Reservoirs*. Tech. rep., PETSOC-08-03-49, http://dx.doi.org/10.2118/08-03-49.

Chien, T., Caudle, S., 1994. *Improved Analytical Solution for Real Gas Flow in Porous Media*. Tech. rep., SPE-27665-MS, http://dx.doi.org/10.2118/27665-MS.

Cutler J. Morris, C., 2009. *Dictionary of Energy (Expanded Edition)*. www.knovel.com.

Daintith, John Martin, E., 2010. *Dictionary of Science (6th Edition)*. www.knovel.com.

Doornhof, D., Kristiansen, T. G., Nagel, N. B., Pattillo, P. D., Sayers, C., 2006. *Compaction and Subsidence*. Tech. rep., Schlumberger.

Earlougher, R. C., 1977. *Advances in Well Test Analysis*. Society of Petroleum Engineers.

Economides, M., Buchsteiner, H., Warpinski., N., 1994. *Step-Pressure Test for Stress-Sensitive Permeability Determination*. Tech. rep., SPE-27380-MS, http://dx.doi.org/10.2118/27380-MS.

Everdingen, A. V., Hurst, W., 1949. *Application of the Laplace Transformation to Flow Problems in Reservoirs*. Tech. rep., Society of Petroleum Engineers, http://dx.doi.org/10.2118/949305-G.

Finjord, J., Aadnoy, B. S., 1989. *Effects of the Quadratic Gradient Term in Steady-State and Semisteady-State Solutions for Reservoir Pressure*. Tech. rep., Society of Petroleum Engineers, http://dx.doi.org/10.2118/15969-PA.

Geoscience, 2015. *Unconventional Resources - Passion for Geoscience*. URL `http://www.cgg.com/default.aspx?cid=3501`

Grant, M., Bixley, P. F., 2011. *Geothermal Reservoir Engineering*. Elsevier.

Hussainy, Ramey, Crawford, 1966. *The Flow of Real Gases Through Porous Media*. Tech. rep., SPE-1243-A-PA, http://dx.doi.org/10.2118/1243-A-PA.

Jelmert, T., 2015. *Thesis Supervisor - Private Communication*.

Jelmert, T., Fall 2014. *TPG4235 - Well Testing, Advanced Course*.

Jelmert, T., Selseng, H., 1998. *Horner plot aids analysis in stress-sensitive reservoirs*. Tech. rep., Oil and Gas Journal.

Jelmert, T. A., 2013. *Introductory Well Testing*. Tom Aage Jelmert and bookboon.com.

Jelmert, T. A., 2014. *Use of Composite Elastic Modulus to Predict Inflow Performance*. Tech. rep., Norwegian University of Science and Technology, Saga Petroleum.

jiao Xiao, X., Sun, H., Han, Y., Yang., J., 2009. *Dynamics Characteristics Evaluation Methods of Stress-Sensitive Abnormal High Pressure Gas Reservoir*. Tech. rep., SPE-124415-MS, http://dx.doi.org/10.2118/124415-MS.

Kikani, J., Pedrosa, O. A., 1991. *Perturbation Analysis of Stress-Sensitive Reservoirs (includes associated papers 25281 and 25292*. Tech. rep., SPE-20053-PA, http://dx.doi.org/10.2118/20053-PA.

Kohlhaas, C., Miller, F., 1969. *Rock-Compaction and Pressure-Transient Analysis with Pressure-Dependent Rock Properties*. Tech. rep., Society of Petroleum Engineers, http://dx.doi.org/10.2118/2563-MS.

Lee, J., 1982. *Well Testing*. Society of Petroleum Engineers of AIME.

Liehui, Z., Jingjing, G., Qiguo, L., 2010. *A well test model for stress-sensitive and heterogeneous reservoirs with non-uniform thicknesses*. Tech. rep., China University of Petroleum (Beijing) and Springer-Verlag Berlin Heidelberg, DOI 10.1007/s12182-010-0103-z.

Lillehammer, K. B., 2014. *Stress-Sensitive Reservoirs and the Effect of Pressure Dependent Variables* . Master's thesis, NTNU.

Mathworks, 2015. *Exponential Integral*.
URL `http://se.mathworks.com/help/symbolic/ei.html`

Matthews, C. S., Russell, D. G., 1967. *Pressure buildup and flow tests in wells*. Society of Petroleum Engineers.

Pedrosa, O., 1986. *Pressure Transient Response in Stress-Sensitive Formations*. Tech. rep., SPE, http://dx.doi.org/10.2118/15115-MS.

Ren, J., Guo, P., 2014. *A New Mathematical Model for Pressure Transient Analysis in Stress-Sensitive Reservoirs*. Tech. rep., http://dx.doi.org/10.1155/2014/485028.

Renpu, W., 2011. *Advanced Well Completion Engineering*. www.knovel.com.

R.Raghavan, Scorer, J., F.G.Miller, 1972. *An Investigation by Numerical Methods of the Effect of Pressure-Dependent Rock and Fluid Properties on Well Flow Tests*. Tech. rep., SPE 2617, http://dx.doi.org/10.2118/2617-PA.

Snoeks, J., 2015. *Oil and Gas Flow Rates - How to Determine if a Well's Daily Production Range is Fair*.
URL `http://www.undervaluedequity.com/Oil-and-Gas-Flow-Rates-How-to-Determine-if-a-Well's-Daily-Production-Range-is-Fair.html`

Srigutomo, W., 2014. *Numerical Inverse Laplace Transform using Gaver-Stehfest method*.
URL `http://www.mathworks.com/matlabcentral/fileexchange/9987`

Stewart, G., 2011. *Well Test Design and Analysis*. Pennwell Corp, Har/Cdr edition.

Sun, H., Branch, L., 2007. *Study on Productivity Evaluation and Performance Prediction Method of Overpressured, Stress-Sensitive Gas Reservoirs*. Tech. rep., SPE-108451-MS, http://dx.doi.org/10.2118/108451-MS.

Vairogs, J., Heam, C. L., Dareing, D. W., Rhoades, V. W., 1971. *Effect of Rock Stress on Gas Production From Low-Permeability Reservoirs*. Tech. rep., SPE-3001-PA, http://dx.doi.org/10.2118/3001-PA.

WolframMathworld, 2015.
URL `http://mathworld.wolfram.com/LaplaceTransform.html`

Wyble, D., 1958. *Effect of Applied Pressure on the Conductivity, Porosity and Permeability of Sandstone*. Tech. rep., SPE-1081-G, http://dx.doi.org/10.2118/1081-G.

Zhang, M., Ambastha, A., 1994. *New Insight in Pressure-Transient Analysis for Stress-Sensitive Reservoirs*. Tech. rep., Society of Petroleum Engineers, http://dx.doi.org/10.2118/28420-MS.

Zhang, M. Y., 1994. *Pressure Transient Analysis For Stress-Sensitive Reservoirs*. Master's thesis, Department of Mining, Metallurgical and Petroleum Engineering, Edmonton, Alberta, National Library of Canada.

Appendix A

Additional calculations

Pressure dependent parameter relations

$$\gamma = \frac{1}{k}\frac{dk}{dp}, c = \frac{1}{\rho}\frac{d\rho}{dp} = \frac{1}{B^{-1}}\frac{dB^{-1}}{dp}, \upsilon = \frac{1}{\mu}\frac{d\mu}{dp}, \xi = \frac{1}{h}\frac{dh}{dp} \tag{A.1}$$

$$T(p) = \frac{kh\rho}{\mu} = \frac{k_{ref}e^{\gamma(p-p_{ref})}h_{ref}e^{\xi(p-p_{ref})}\rho_{ref}e^{-c(p-p_{ref})}}{\mu_{ref}e^{\nu(p-p_{ref})}} \tag{A.2}$$

$$= \frac{k_{ref}h_{ref}\rho_{ref}}{\mu_{ref}}e^{(\gamma+c+\xi-\upsilon)(p-p_{ref})} \tag{A.3}$$

Deriving the basic relationship based on elasticity modulus

$$\tau_D = \frac{1}{T_n}\frac{dT_n}{dp} \tag{A.4a}$$

$$\int_{p_i}^{p} dp = \frac{1}{\tau}\int_{1}^{T_n}\frac{1}{T_n}dT_n \tag{A.4b}$$

$$p - p_i = \frac{1}{\tau}\ln T_n(p) \tag{A.4c}$$

$$T_n = 1 - \Delta T_n = e^{-\tau(p_i - p)} \tag{A.4d}$$

$$\ln T_n = \ln(1 - \Delta T_n) = -\tau(p_i - p) \tag{A.4e}$$

$$(p_i - p) = -\frac{1}{\tau}\ln T_n = - - \frac{1}{\tau}\ln(1 - \Delta T_n) \tag{A.4f}$$

Dimensionless inner boundary conditions in terms of p_D

$$q_{sc}B\left(p\right) = q_{sf} \tag{A.5a}$$

$$\frac{V_{osc}}{t}\frac{V_{ores}(p)}{V_{osc}} = \frac{V_{ores}(p)}{t} \tag{A.5b}$$

$$\rho_{nsf}(p) = \frac{M/V_{ores}(p)}{M/V_{ores}(p_i)} = \frac{V_{ores}(p_i)}{V_{ores}(p)} \tag{A.5c}$$

$$\rho_{nsf}(p)B(p) = \frac{V_{ores}(p_i)}{V_{ores}(p)}\frac{V_{ores}(p)}{V_{osc}} = \frac{V_{ores}(p_i)}{V_{osc}} = B_i \tag{A.5d}$$

Deriving the E_i solution

From the relationship given by equation A.4f

$$\frac{2\pi k_i h_i}{q_{sc}\mu_i B}d\Delta p = -\frac{2\pi k_i h_i}{q_{sc}\mu_i B}\ln T_n = -\frac{1}{\tau_D}\ln(1-\Delta T_n) \tag{A.6a}$$

From the relationship given by equation A.4d

$$\Delta T_n = e^{-\tau(p_i-p)} - 1 \tag{A.6b}$$

$$\Delta T_n = e^{-\frac{\tau q \mu_j}{2\pi k_i h_i}} - 1 \tag{A.6c}$$

$$1 + \Delta T_n = e^{-\tau_D p_D} \tag{A.6d}$$

$$\ln\left(1+\Delta T_n\right) = -\tau_D p_D \tag{A.6e}$$

$$p_D = -\frac{1}{\tau_D}\ln\left(1+\Delta T_n\right) \tag{A.6f}$$

Appendix B

MATLAB code

This appendix includes a few of the MATLAB codes used for the given study. All solutions and plots have been found using the codes presented below or similar ones with modifications to fit the problem.

Build up solution for Horner plot for Kikani and Petrosa solution, the new solution using the build in Ei function and the new solution using Laplace transform. The latter calls for the Gaver Stehfest algorithm (MATLAB code listed below this one) which again find the Laplace equation expressed by Bessel function (MATLAB code further below -Bessel solution for stress-sensitive case) assuming no storage and skin.

```
%% %Ei solution from Kikani and Pedrosa with several td values
clear all
close all

tpD=10000;
yD = [0.01 0.15 0.20 0.25 0.30 0.35];
Delta = [10 25 50 100 250 500 1000 2500 5000 10000];

for i = 1:length(yD)
    for j=1:length(Delta);
        timeax(j)=(tpD+Delta(j))/Delta(j);
        pds(i,j)= -1/yD(i)*log(1-(yD(i)/2)*expint(1/(4*(tpD+Delta(j))))+(
    yD(i)/2)*expint(1/(4*Delta(j))));
        if imag(pds(i,j))~=0;
            pds(i,j)=NaN;
        end
    end
end

```

```
%% Ei solution for new derived model
tpd= 10000;
tauD = 0.25;
rd=1;
Delta = [10 25 50 100 250 500 1000 2500 5000 10000];

for j=1:length(Delta);
    time(j)=(tpd+Delta(j))/Delta(j);
    z1(j)=rd^2/(4*(tpd+Delta(j)));
    z2(j)=rd^2/(4*(Delta(j)));
    DTn1(j) = -(tauD/2)*-ei(-z1(j));
    DTn2(j)= -(tauD/2)*-ei(-z2(j));
    DTnT(j)=DTn1(j)-DTn2(j);
    pDBU(j)=-(1/tauD)*log(1+DTnT(j));
    if imag(pDBU(j))~=0;
        pDBU(j)=NaN
    end
end


%%Laplace solution for new derived model

L=10;
tauDD=0.25;
tpD2=10000;

Dt = [10 25 50 100 250 500 1000 2500 5000 10000];

for l=1:length(Dt)
    P_BU1(l)=gavsteh('funbessel',tpD2+Dt(l),L);
    P_BU2(l)=gavsteh('funbessel',Dt(l),L);
    timeaxi(l)=(tpD2+Dt(l))/Dt(l);
    pDD(l)=(-1/tauDD)*log(1-(tauDD)*P_BU1(l)+(tauDD)*P_BU2(l));
end
```

The Gaver-Stehfest algorithm giving an approximate solution to inverse Laplace transforms back to time domain, Srigutomo (2014).

```
%  ilt=gavsteh(funname,t,L)
%
%    funname        The name of the function to be transformed.
%    t              The transform argument (usually a snapshot of time).
%    ilt              The value of the inverse transform
%    L               number of coefficient ---> depends on computer word
    length used
%                    (examples: L=8, 10, 12, 14, 16, so on..)
```

```
%
%  Wahyu Srigutomo
%  Physics Department, Bandung Institute of Tech., Indonesia, 2006
%  Numerical Inverse Laplace Transform using Gaver-Stehfest method
%
%Refferences:
% 1. Villinger, H., 1985, Solving cylindrical geothermal problems using
%   Gaver-Stehfest inverse Laplace transform, Geophysics, vol. 50 no. 10 p.
%   1581-1587
% 2. Stehfest, H., 1970, Algorithm 368: Numerical inversion of Laplace transform,
%    Communication of the ACM, vol. 13 no. 1 p. 47-49
%
% Simple (and yet rush) examples included in functions fun1 and fun2 with
% their comparisons to the exact value (use testgs.m to run the examples)
function ilt=gavsteh(funname,t,L)
nn2 = L/2;
nn21= nn2+1;

for n = 1:L
    z = 0.0;
  for k = floor( ( n + 1 ) / 2 ):min(n,nn2)
        z = z + ((k^nn2)*factorial(2*k))/ ...
            (factorial(nn2-k)*factorial(k)*factorial(k-1)* ...
            factorial(n-k)*factorial(2*k - n));
    end
    v(n)=(-1)^(n+nn2)*z;
end

sum = 0.0;
ln2_on_t = log(2.0) / t;
for n = 1:L
    p = n * ln2_on_t;
    sum = sum + v(n) * feval(funname,p);
end
  ilt = sum * ln2_on_t;
```

The Bessel expression in Laplace space for the line source solution. C_D and S can be changed as desired.

```
function f=linesourcebessel(p)

Cd =100;
S=0;
a=sqrt(p);
```

```
% Line source solution
f=(besselk(0,a)+S)./(p*(1+Cd.*a*(besselk(0,a))+S.*Cd.*a));
```

The Bessel expression in Laplace space for the stress-sensitive solution. C_D and S can be changed as desired.

```
function f=funbesselCS(p)

Cd =100;
S=0;
a=sqrt(p);
%Stress-sensitive solution
f=(besselk(0,a)+S*a*besselk(1,a))./(p*(a*besselk(1,a)+a*Cd*(besselk(0,a)+S
    *a*besselk(1,a))));
```

The time domain solution, which runs the Bessel expression solutions through the Stefhest algorithm and thereby retrieves time domain values.The time domain solutions are found and can be plotted against desired τ_D value/values.

```
%Solution including storage and skin for both line source solution and
%analytical stress-sensitive solution. Using Gaver-Stehfest inverse
    Laplace
%transform algorithem to get solution in time domain.
clear all
close all

L=10;

tauD= [0.1  0.2];
tD = [10 100 250 500 1000 2500 5000 10000 100000 10000000 100000000];


for l=1:length(tD)
     % Storage 0 skin 0
    pD1(l)=gavsteh('linesourcebessel1',tD(l),L);
          if imag(pD1(l))~=0;
           pD1(l)=NaN;
           end
    dTnCS1(l)=gavsteh('funbesselCS1',tD(l),L);
    for k=1:length(tauD)
        pDCS1(l,k)=-1/tauD(k)*log(1-tauD(k)*dTnCS1(l));
        if imag(pDCS1(l,k))~=0;
            pDCS1(l,k)=NaN;
        end
    end
    %Storage 100 skin 20
```

```
    pD(1)=gavsteh('linesourcebessel',tD(1),L);
          if imag(pD(1))~=0;
          pD(1)=NaN;
          end
    dTnCS(1)=gavsteh('funbesselCS',tD(1),L);
    for k=1:length(tauD)
        pDCS(1,k)=-1/tauD(k)*log(1-tauD(k)*dTnCS(1));
        if imag(pDCS(1,k))~=0;
            pDCS(1,k)=NaN;
        end
    end

end

datacheck= [pD' dTnCS' pD1' dTnCS1']

plot1 = loglog(tD, pD1,'r','LineWidth',1.5);
hold on
plot2 = loglog(tD, pDCS1,'b','LineWidth',1.5);
hold on
plot3 = loglog(tD, pD,'-*r','LineWidth',1.5);
hold on
plot4 = loglog(tD, pDCS,'-*b','LineWidth',1.5);
hold on


title('Drawdown with Wellbore storage and Skin','FontSize',24 )
grid on
xlabel('t_D','FontSize',18)
ylabel('p_D','FontSize',18)
set(gca, 'FontSize',18)
legend('Homogeneous solutions, C_D = 0, S = 0 ','Stress-sensitive
    solutions, C_D = 0, S = 0', 'Homogeneous solutions, C_D = 100, S = 0',
     'Stress-sensitive solutions, C_D = 100, S = 0');

str = {'\tau_D = 0', 'r_D = 1'};
annotation('textbox', [.15 .8, .1, .1], 'String', str,'FontSize',18,'
    BackgroundColor',[0.9 0.9 0.9]);
hold all
```